01 Jul 2022

Derivation and Analysis of a Discrete Predator–Prey Model

Sabrina H. Streipert

Gail S.K. Wolkowicz

Martin Bohner
Missouri University of Science and Technology, bohner@mst.edu

Society for
Mathematical
Biology

Derivation and Analysis of a Discrete Predator–Prey Model

Sabrina H. Streipert[1] · **Gail S.K. Wolkowicz**[1] · **Martin Bohner**[2]

Abstract

We derive a discrete predator–prey model from first principles, assuming that the prey population grows to carrying capacity in the absence of predators and that the predator population requires prey in order to grow. The proposed derivation method exploits a technique known from economics that describes the relationship between continuous and discrete compounding of bonds. We extend standard phase plane analysis by introducing the next iterate root-curve associated with the nontrivial prey nullcline. Using this curve in combination with the nullclines and direction field, we show that the prey-only equilibrium is globally asymptotic stability if the prey consumption-energy rate of the predator is below a certain threshold that implies that the maximal rate of change of the predator is negative. We also use a Lyapunov function to provide an alternative proof. If the prey consumption-energy rate is above this threshold, and hence the maximal rate of change of the predator is positive, the discrete phase plane method introduced is used to show that the coexistence equilibrium exists and solutions oscillate around it. We provide the parameter values for which the coexistence equilibrium exists and determine when it is locally asymptotically stable and when it destabilizes by means of a supercritical Neimark–Sacker bifurcation. We bound the amplitude of the closed invariant curves born from the Neimark–Sacker bifurcation as a function of the model parameters.

Keywords Difference equations · Predator–prey · Neimark–Sacker bifurcation · Global stability · Lyapunov function

✉ Sabrina H. Streipert
streipes@mcmaster.ca

Gail S.K. Wolkowicz
wolkowic@mcmaster.ca

Martin Bohner
bohner@mst.edu

[1] Department of Mathematics and Statistics, McMaster University, 1280 Main St. W., Hamilton, ON L8S4K1, Canada

[2] Department of Mathematics and Statistics, Missouri S&T, 400 W 12th St., Rolla, MO 65409, USA

1 Introduction

Mathematical models describing interactions of populations are essentially based on one or more of the three main relationships: mutualism, competition, and predation. A popular, but simple example of continuous predator–prey systems is the Lotka–Volterra model. The model was formulated independently by Lotka (1920) and Volterra (1926). While Lotka applied this system of ordinary differential equations to a chemical reaction and later to a plant population with a dependent species (Lotka 1920), Volterra used the periodic solutions of this predator–prey system to explain oscillatory fish catches in the Adriatic (Kingsland 1995). The model assumes that the prey population grows exponentially in the absence of predators and the predator population decays exponentially in the absence of prey. The contribution of the prey to the growth of the predator population is assumed to be proportional to the product of the size of the predator population and the size of the prey population. Similarly, the decline in the size of the prey population in the presence of predators is assumed to be proportional to the product of the sizes of the two populations. The classical and widely studied Lotka–Volterra model is then given by

$$x' = rx - \alpha xy, \quad y' = -dy + \gamma xy, \tag{1}$$

where $r > 0$ is the growth rate (in the absence of the predator) and $d > 0$ represents the decay rate of the predator in the absence of the prey. The positive parameters α and γ determine the consumption rate and consumption-energy rate, respectively. The coexistence equilibrium of (1) is a center, and a family of periodic orbits oscillates about the coexistence equilibrium with an oscillation frequency that is more rapid for larger prey reproduction rates and larger predator mortality rates. A criticism of the model is the structural instability, since a small change in the equations can eliminate the existence of periodic orbits (Kot 2001).

Another criticism of (1) is the assumption of exponential growth for the prey population. This has also been criticized for single species models as resources are generally limited. Consequently, Verhulst (1838) introduced the so-called logistic growth model, assuming limited resources and resulting in convergence to a positive carrying capacity. It is reasonable to assume a similar convergence behavior for the prey population in the absence of the predator rather than the assumption of unbounded growth as in the classical Lotka–Volterra model.

Thus, assuming logistic growth for the prey in the absence of the predator, one obtains the modified predator–prey model

$$x' = rx \left(1 - \frac{x}{K}\right) - \alpha xy, \quad y' = -dy + \gamma xy, \tag{2}$$

where the parameters r, α, d, and γ have the same biological interpretation as in (1). However, to account for intra-specific competition among the prey population, the

additional parameter $K > 0$ that represents the carrying capacity of the prey population was introduced. The dynamics of (2) differs from the behavior of solutions of the classical Lotka–Volterra model (1). In contrast to (1), where solutions cycle periodically about the coexistence equilibrium with x-amplitude and y-amplitude dependent on initial conditions, using the Bendixson–Dulac negative criterion (Kot 2001), it can be proven that no periodic orbits exist for (2). If the prey consumption-energy rate of the predator γ satisfies $\gamma > \frac{d}{K}$, then the coexistence equilibrium is globally asymptotically stable. If, however, $\gamma < \frac{d}{K}$, then the prey-only equilibrium is globally asymptotically stable (see Brauer and Castillo-Chavez 2011). The aim of this work is to formulate a discrete predator–prey model based on the same assumptions as (2).

There are different reasons for using discrete mathematical models. While they are often preferred due to their computational convenience, they are also more appropriate for modelling nonoverlapping generations, such as monocarpic plants and semelparous fish species (see Kot 2001 for more examples). Independent of the motivation, a common method to obtain a recurrence relation, presumably satisfying the same assumptions as an underlying continuous model, is to apply a discretization process, such as the Euler scheme, to an existing continuous model. The justification that, as the stepsize approaches zero, a corresponding continuous model is retrieved is particularly questionable when modeling non-overlapping generations where the step-size represents the generation time. Applying the forward Euler method in the case of the logistic growth model, $x' = rx\left(1 - \frac{x}{K}\right)$, the logistic difference equation, $X_{t+1} = X_t + rX_t\left(1 - \frac{X_t}{K}\right)$, is obtained. However, this discretizaton displays significantly different behavior compared to the behavior of the continuous logistic differential equation. Nevertheless, the application of the Euler scheme to continuous models remains a popular method for formulating discrete models that supposedly satisfy the same assumptions as the underlying continuous model. This technique has also been favored to formulate discrete predator–prey models. See for example (Chen et al. 2013a, b; Choudhury 1992; Fan and Agarwal 2002; He and Li 2014; Wang et al. 2013).

In Zhao et al. (2016), the authors investigate the discrete predator–prey model

$$X_{t+1} = rX_t(1 - X_t) - \alpha X_t Y_t, \quad Y_{t+1} = -dY_t + \gamma X_t Y_t, \qquad (3)$$

that results from applying the Euler scheme to (2) and choosing the carrying capacity $K = 1$. The authors show that if the prey's growth rate, r, and the predator's death rate, d, are both positive and less than 1, then the trivial solution is asymptotically stable. For other parameter values, the prey-only equilibrium is locally asymptotically stable, and conditions for the local stability of the coexistence equilibrium for which both species survive are provided, but often require nonlinear relations between parameters. Certain parameter combinations result in a flip bifurcation, that is, a period doubling of the coexistence equilibrium as a parameter varies. Another combination of parameter values results in a Neimark–Sacker bifurcation of the coexistence equilibrium as a parameter varies, that is, a closed invariant curve appears when a fixed point changes stability (Guckenheimer and Holmes 1983; Zhang 2006; Wiggins 2003). The analogue of such a bifurcation in continuous models is a Hopf bifurcation. Therefore,

the dynamics of this discretization are different from the dynamics of the continuous model (2). It can even be shown that the model can predict negative population values for some positive parameters and positive initial conditions.

Another common method used to formulate discrete models exploits a Ricker-type structure and prevents solutions from becoming negative. Such a discretization of (2) is then given in Beddington et al. (1975), by

$$X_{t+1} = X_t e^{r\left(1 - \frac{X_t}{K}\right)} - \alpha Y_t, \quad Y_{t+1} = dX_t \left(1 - e^{-\gamma Y_t}\right), \tag{4}$$

with the same interpretation of the parameters as before. That is, r is the prey's growth rate and K is the prey's carrying capacity. Consequently, the intra-specific competition rate is determined by $\frac{r}{K}$. The predation rate of the prey by the predator is α. The parameter d is the death rate of the predator and γ is the energy-conversion rate of predation. The equilibrium $(K, 0)$ of (4) is stable for $r \in (0, 2)$, and for $r > 2$, solutions of (4) are periodic (Beddington et al. 1975). The model further exhibits transcritical, flip, and Neimark–Sacker bifurcations (see Beddington et al. 1975, 1978; May 1974).

Another discretization of (2) was introduced in Din (2013) as

$$X_{t+1} = \frac{rX_t - \alpha X_t Y_t}{1 + \frac{r}{K} X_t}, \quad Y_{t+1} = \frac{\eta Y_t + \gamma X_t Y_t}{1 + \varphi Y_t}, \tag{5}$$

with positive parameter values $r, \alpha, K, \eta, \gamma$, and φ. The interpretation of the model parameters follows the previous interpretations, with the parameter η representing a growth contribution of the predator and φ representing the intra-specific competition in the predator population. However, solutions can take negative values. Although not argued by the authors, but given the structural similarities, we assume this formulation of (5) was motivated by the Beverton–Holt model that is often considered to be a discrete analogue of the continuous logistic growth model (Bohner and Streipert 2016; Bohner and Warth 2007; Brauer and Castillo-Chavez 2011). The authors of Din (2013) prove that if $r, \eta \in (0, 1)$, then the trivial equilibrium is locally asymptotically stable. If $r > 1$, $\eta < 1$, and $\gamma < \frac{\frac{r}{K}(1-\eta)}{r-1}$, then the prey-only equilibrium is locally asymptotically stable. In contrast with (2), the predator-only equilibrium can also be stable if $\eta > 1$ and $r < 1$, and if $r\eta > 1$ and $\varphi \frac{r}{K} \neq \alpha\gamma$, then the coexistence equilibrium (x^*, y^*) is globally asymptotically stable.

A discretization of a predator–prey model that is related to our model was introduced in Liu and Elaydi (2001) as

$$
\begin{aligned}
X_{t+1} &= \frac{(1 + r_1 \varphi_1(h)) X_t}{1 + \varphi_1(h)(a_{11} X_t + a_{12} Y_t)}, \\
Y_{t+1} &= \frac{(1 + r_2 \varphi_2(h) - \varphi_2(h) a_{21} X_t) Y_t}{1 + \varphi_2(h) a_{22} Y_t}.
\end{aligned}
\tag{6}
$$

The model was derived by applying a modified Mickens discretization scheme (Mickens 1989, 1994a; Mickens and Smith 1990; Mickens 1994b) to the continuous model

$$x' = x(r_1 - a_{11}x_t - a_{21}y), \quad y' = y(r_2 - a_{21}x - a_{22}y).$$

For $a_{12} > 0$ and $a_{21} < 0$, a predator–prey relation was obtained. We note that, if additionally $a_{22} = 0$, then (2) is obtained. The authors, however, focus their stability results on the cases of competition and cooperation between the species, leaving the global analysis of the predator–prey difference equation an open problem. We emphasize that our derivation comes from first principles, based directly on the assumptions on population growth and decline, and not from discretizing a continuous model as in Liu and Elaydi (2001).

In this work, we derive a discrete predator–prey model based on the same assumptions as (2). Instead of applying a discretization scheme, we derive the two-species discrete model directly using first principles based on the assumptions. Starting out with a single species model, we first assume that a population at time $t + 1$ is a multiple of the population at time t, considering both the growth and the decline processes. After establishing a general description of how a population changes over a cycle, based on its growth and decline contribution, we then take into consideration the model assumptions from (2) on how the prey and predators interact to formulate a discrete predator–prey model in Sect. 2 that is analyzed in Sect. 3. We compare its dynamics with that of the continuous model (2) and highlight the similarities. In both models, if the product of the consumption-energy rate of the predator and the carrying capacity is smaller than the death rate of the predator, the prey-only equilibrium is globally asymptotically stable. If, however, this product is bigger than the death rate of the predator, the two models differ slightly, as the asymptotic stability of the coexistence equilibrium only holds in the discrete model when the parameters fall within a certain interval. We illustrate our results with figures produced using Matlab MATLAB (2020). We conclude the manuscript by summarizing the dynamic behavior of our discrete predator–prey model and highlight its similarities and differences compared to the continuous analogue (2).

2 Model Derivation

In this section, we propose a new derivation method to formulate discrete multi-species models. We specifically apply this derivation technique to describe a predator–prey relationship. Prior to formulating the two-species model, we make a crucial observation regarding single population models. The derivation of our model is based upon the assumption that the population at time $t + 1$ can be described as a factor $f(t)$ of the population at time t, that is, $X_{t+1} = f(t)X_t$. The (possibly time-dependent) factor $f(t)$ is determined by growth and decline processes. Thus, we may express the population at time $t + 1$ as

$$X_{t+1} = f(t)X_t = \frac{1 + p(t)}{1 + q(t)}X_t, \tag{7}$$

where $p(t)$ captures the processes contributing to the increase of the population and $q(t)$ captures the processes contributing to the decrease in the population between time steps t and $t + 1$. In fact, (7) is related to the solution of the continuous population model

$$x'(t) = (p(t) - q(t))x(t), \tag{8}$$

where p, q describe the growth and decline, respectively, for infinitesimal time steps. The solution of (8) satisfies

$$x(t + 1) = \frac{e^{\int_t^{t+1} p(s)\,ds}}{e^{\int_t^{t+1} q(s)\,ds}} x(t) = \tilde{f}(t)x(t). \tag{9}$$

Equation (9) reveals similarities with the expression in (7), as the population at time $t + 1$ is a multiple of the population at time t. The factor in (9) can be expressed as a ratio of exponential terms, where the numerator describes the growth contribution and the denominator the decay. Recalling that

$$\lim_{n \to \infty} \left(1 + \frac{F}{n}\right)^n = e^F, \tag{10}$$

we argue that if the processes were to take place discretely, $n = 1$ and e^F would be replaced by $1 + F$, giving an additional interpretation of the model construction in (7). The same observation is commonly applied in economics, where zero-coupon bonds with only one payment P of interest are modelled by $P_{t+1} = (1 + r)P_t$, where r is the annual interest rate, while bonds with monthly coupons are modelled by $P_{t+1} = \left(1 + \frac{r}{12}\right)^{12} P_t$. Continuous payments then lead to $P_{t+1} = e^r P_t$.

The derivation of (7) can easily be extended to consider the interaction of several species X_i, for $i = 1, 2, \ldots, k$. In this case, species X_i at time $t + 1$ is expressed by

$$X_i(t + 1) = \frac{1 + p_i(t, X_1, X_2, \ldots, X_k)}{1 + q_i(t, X_1, X_2, \ldots, X_k)} X_i(t).$$

In our case, X_i, for $i = 1, 2$, represents the prey and the predator. We assume, as in (2), that the prey population increases with a constant growth rate $r > 0$. Thus, the growth contribution is $p(t) = r$. We also assume that competition and predation are the factors responsible for any decline in the prey population. More precisely, for the prey population, we consider

$$q(t) = \frac{r}{K} X_t + \alpha Y_t,$$

where the carrying capacity is given by $K > 0$ and the intra-specific competition for the prey population is given by $\frac{r}{K}$. Thus, $\frac{r}{K} X_t$ captures the decline due to competition,

and αY_t, with predation rate $\alpha > 0$, captures the decline due to predation. We therefore obtain the recurrence for the prey as

$$X_{t+1} = \frac{1+r}{1 + \frac{r}{K} X_t + \alpha Y_t} X_t. \tag{11}$$

It is worth noting that in the absence of a predator, the prey recurrence in (11) collapses to $X_{t+1} = \frac{(1+r)X_t}{1 + \frac{r}{K} X_t}$, which is equivalent to the Beverton–Holt model (Beverton and Holt 1957). Solutions of the Beverton–Holt model are known to converge to K for positive initial conditions (Beverton and Holt 1957; Bohner and Warth 2007). It is for this reason that the model parameter K is often referred to as the "carrying capacity".

For the predator population, we assume, as in (2), that the predator population declines with a constant rate $d > 0$, resulting in $q(t) = d$, and the growth rate depends on consumption of the prey, and hence is proportional to the size of the prey population. We therefore consider $p(t) = \gamma X_t$, where $\gamma > 0$ is the prey consumption-energy rate of the predator. This results in the recurrence for the predator

$$Y_{t+1} = \frac{1 + \gamma X_t}{1 + d} Y_t. \tag{12}$$

Combining (11) and (12), we arrive at the discrete predator–prey model

$$X_{t+1} = f(X_t, Y_t), \quad Y_{t+1} = g(X_t, Y_t), \quad t \geq 0$$
$$\text{with} \quad f(x, y) = \frac{(1+r)x}{1 + \frac{r}{K} x + \alpha y}, \quad g(x, y) = \frac{(1 + \gamma x)y}{1 + d}, \tag{13}$$

where the initial conditions X_0, Y_0 are assumed to be nonnegative and the parameters r, K, α, γ, d are assumed to be positive.

Remark 1 Choosing the parameters in (6), derived in Liu and Elaydi (2001), as

$$a_{22} = 0, \quad r_1 \varphi_1(h) = r, \quad a_{11} \varphi_1(h) = \frac{r}{K},$$
$$a_{12} \varphi_1(h) = \alpha, \quad r_2 \varphi_2(h) = \frac{-d}{1+d}, \quad a_{21} \varphi_2(h) = \frac{-\gamma}{1+d},$$

results in our proposed model (13).

Remark 2 The model clearly satisfies the *axiom of parenthood* (Edelstein-Keshet 1988; Hutchinson 1978), that is, every organism must have parents. More precisely, this means that if $X_0 = 0$, then $X_t = 0$ for all $t \geq 0$ and similarly, if $Y_0 = 0$, then $Y_t = 0$ for all $t \geq 0$.

The partial derivatives of the functions f and g in (13) satisfy

$$f_x = \frac{K^2(1+r)(1 + \alpha y)}{(K + rx + \alpha K y)^2} > 0, \quad f_y = -\frac{\alpha K^2(1+r)x}{(K + rx + \alpha K y)^2} < 0,$$
$$g_x = \frac{\gamma y}{1+d} > 0, \quad g_y = \frac{1 + \gamma x}{1+d} > 0,$$

where $h_u = \frac{\partial h}{\partial u}$ for $h \in \{f, g\}$ and $u \in \{x, y\}$. Hence, f is monotone in each variable, as it increases in x and decreases in y. Similarly, g is monotone since it increases in each variable. However, (13) is not monotone in the sense of Smith (see Hirsch and Smith 2005; Smith and Thieme 2013), because f_y and g_x do not necessarily have the same sign. This property is called sign-symmetry and is required for the system to be monotone in the sense of Smith.

We remind the reader that while $X_{t+1} = f(X_t, Y_t)$ is increasing in X_t, it does not imply that the sequence of iterates, X_t, is increasing. In fact, X_t is increasing if the forward operator, $\Delta X_t = X_{t+1} - X_t$ is positive. For system (13), the forward operators are

$$\Delta X_t = X_{t+1} - X_t = \frac{(1+r)X_t}{1 + \frac{r}{K}X_t + \alpha Y_t} - X_t = X_t \frac{r\left(1 - \frac{X_t}{K}\right) - \alpha Y_t}{1 + \frac{r}{K}X_t + \alpha Y_t}$$
$$= \frac{X_{t+1}}{1+r}\left[r\left(1 - \frac{X_t}{K}\right) - \alpha Y_t\right] \tag{14}$$

and

$$\Delta Y_t = Y_{t+1} - Y_t = \frac{(1 + \gamma X_t)Y_t}{1 + d} - Y_t = Y_t \frac{\gamma X_t - d}{1 + d}. \tag{15}$$

From (14), we see that $X_t > 0$ is increasing if and only if $r\left(1 - \frac{X_t}{K}\right) > \alpha Y_t$, since $X_{t+1} > 0$ for $X_t > 0$. Thus, if (X_t, Y_t) is above the line

$$y = \ell(x) := \frac{r}{\alpha K}(K - x), \tag{16}$$

$Y_t > \ell(X_t)$, then the sequence of iterates, X_t, is decreasing and if $Y_t < \ell(X_t)$, then X_t is increasing. Similarly, from (15) it follows that Y_t is increasing as long as $\gamma X_t > d$ and decreasing if $\gamma X_t < d$.

The model just derived differs from the existing models mentioned in the introduction. Although (13) was derived under the same assumptions concerning growth and decline as the continuous model (2), it differs from existing discretizations of (2). In particular, (13) was not derived by applying a discretization scheme, such as the forward Euler method. Instead it was derived from the assumptions, based on first principles.

We remind the reader that in the absence of the predator, (13) is a single-species model of the form

$$X_{t+1} = \frac{(1+r)X_t}{1 + \frac{r}{K}X_t}.$$

This is the Beverton–Holt model, which can be understood as a discretization of the logistic differential equation (Bohner et al. 2007; Brauer and Castillo-Chavez 2011), and has been extended to quantum calculus (Bohner and R 2013; Bohner and Streipert

2017) and time scales (Bohner and Warth 2007). In the presence of the predator, (13) has the corresponding expression in time scales notation

$$x^\Delta = x^\sigma (a - cx - by), \quad y^\Delta = y(dx - e).$$

This model expression differs from existing predator–prey models on time scales (see Fazly and Hesaaraki 2008a, b; Zhang et al. 2008).

3 Model Dynamics

We consider (13) with $r, K, \alpha, \gamma, d > 0$ and nonnegative initial conditions X_0, Y_0. The first lemma follows immediately from the model structure and its proof is omitted. The proofs of the other lemmas, propositions, and theorems in this section are collected in the Appendix.

Lemma 1 *Solutions of* (13) *with nonnegative initial conditions remain nonnegative. If* $X_0 = 0$, *then* $X_t = 0$ *for all* $t \geq 0$. *If* $Y_0 = 0$, *then* $Y_t = 0$ *for all* $t \geq 0$. *If* $X_0 > 0$ *and* $Y_0 \geq 0$, *then* $X_t > 0$ *for all* $t \geq 0$. *If* $X_0 \geq 0$ *and* $Y_0 > 0$, *then* $Y_t > 0$ *for all* $t \geq 0$.

Lemma 2 *Solutions of* (13) *with nonnegative initial conditions are bounded for* $t \geq 0$. *Additionally,* $X_t \in [0, \max\{X_0, K\}]$ *for all* $t \geq 0$. *If* $X_t < K$ *for some* $T \geq 0$, *then* $X_t < K$ *for all* $t \geq T$, *and if* $X_t > K$, *then either* $\{X_t\}$ *decreases monotonically to* K *or there exists* T *such that* $X_t \leq K$ *for all* $t \geq T$.

Model (13) is a biologically well-posed system, since it satisfies the axiom of parenthood, solutions with nonnegative initial conditions remain nonnegative by Lemma 1, and solutions are bounded by Lemma 2. This is in contrast with some existing discrete predator–prey models, where the prey population at time $t + 1$, X_{t+1}, is defined by a subtraction dependent on the predator population at time t, Y_t. Predator–prey models with a prey equation of the form $X_{t+1} = X_t(a - bX_t) - cX_tY_t$ with $a, b, c > 0$ require additional model assumptions to prevent solutions from becoming negative. Recent predator–prey models that may give rise to negative population levels have been discussed for example in Kangalgil and Isik (2020), Khan et al. (2020), Rana (2019) and Rozikov and Shoyimardonov (2020).

To study the dynamics of the predator–prey model that we introduced, we observe that its equilibria are given by

$$E_0 = (0, 0), \quad E_K = (K, 0), \quad E^* = (x^*, y^*) = \left(\frac{d}{\gamma}, \frac{r(\gamma K - d)}{\alpha \gamma K} \right), \quad (17)$$

where the coexistence equilibrium, E^*, makes sense biologically only if $\gamma K > d$.

Remark 3 The equilibria in (17) are identical to the equilibria of the continuous model (2). The equilibrium solutions of the common discretization (3) are also the same. However, (3) does not satisfy the axiom of parenthood and can predict negative solutions, unlike our model (13).

The behavior of solutions with initial conditions on the boundary of the positive quadrant is fully determined in the following lemma.

Lemma 3 *Consider* (13) *with initial conditions* (X_0, Y_0).

(a) If $X_0 = 0$ and $Y_0 \geq 0$, then (X_t, Y_t) converges to E_0.
(b) If $Y_0 = 0$ and $X_0 > 0$, then (X_t, Y_t) converges to E_K.

To investigate the behavior of solutions with positive initial conditions, we linearize (13) at $(\hat{X}, \hat{Y})$, to obtain,

$$\mathbf{Z}_{t+1} = J\mathbf{Z}_t,$$

where $\mathbf{Z}_t = (X_t, Y_t)$ and

$$J = \begin{bmatrix} \frac{(1+r)(1+\alpha\hat{Y})}{(1+\frac{r}{K}\hat{X}+\alpha\hat{Y})^2} & \frac{-(1+r)\alpha\hat{X}}{(1+\frac{r}{K}\hat{X}+\alpha\hat{Y})^2} \\ \frac{\gamma\hat{Y}}{1+d} & \frac{1+\gamma\hat{X}}{1+d} \end{bmatrix}. \tag{18}$$

Theorem 4 *Consider* (13) *with positive initial conditions. Then the following holds:*

(a) E_0 is unstable.
(b) If $d \geq \gamma K$, then E_K is locally asymptotically stable. If $d < \gamma K$, then E_K is unstable.
(c) If $d < \gamma K < (1+2d)$, then E^* is locally asymptotically stable. If $\gamma K > 1 + 2d$, then E^* is unstable. If $d > \gamma K$, then E^* is not biologically relevant since $y^* < 0$.

Remark 4 By (15), $\Delta Y_t = g(X_t)Y_t$ with $g(X_t) = \frac{\gamma X_t - d}{1+d}$, so that $g(K)$ is the (discrete) maximal rate of change/per-capita growth rate of the predator. Since $X_t \leq K$ for $X_0 \in [0, K]$, $g(K)$ is the maximal rate of change of the predator. The conditions of Theorem 4 can therefore be expressed equivalently in terms of the maximal rate of change of the predator, since

$$\gamma K \leq d \iff \frac{\gamma K}{1+d} \leq \frac{d}{1+d} \iff \frac{\gamma K - d}{1+d} \leq 0 \iff g(K) \leq 0,$$

$$\gamma K \leq 1 + 2d \iff \frac{\gamma K}{1+d} \leq 1 + \frac{d}{1+d} \iff \frac{\gamma K - d}{1+d} \leq 1 \iff g(K) \leq 1. \tag{19}$$

Thus, if the maximal rate of change of the predator is non-positive, that is, $g(K) \leq 0$, then E_K is asymptotically stable and the predator goes extinct for small initial values. If the maximal rate of change of the predator is positive, but less than one, that is, $0 < g(K) < 1$, then the coexistence equilibrium is asymptotically stable.

As for the continuous model (2), the asymptotic stability of (13) depends, therefore, on the sign of $d - \gamma K$. In particular, if $d > \gamma K$, E_K is asymptotically stable. This condition is the same stability condition for the prey-only equilibrium of the continuous model (2), as discussed in (Brauer and Castillo-Chavez 2011). However, in the

continuous model (2), the coexistence equilibrium is globally asymptotically stable as long as $d < \gamma K$, whereas in model (13), it is unstable if $\gamma K > 1 + 2d$. Thus, the system exhibits the paradox of enrichment, that is, the equilibrium destabilizes as the prey carrying capacity increases past a critical value, giving rise to sustained oscillatory behavior, as in the classical Rosenzweig–MacArthur model (Rosenzweig 1971).

While Theorem 4 addresses the local asymptotic stability of the nonnegative equilibria, the remainder of this section investigates the global behavior of solutions. By Lemma 2, solutions remain in the first quadrant for all nonnegative initial conditions. In fact, by Lemma 2, if $X_T \leq K$, then $X_t \leq K$ for all $t \geq T$. We divide the first quadrant into regions based on the component-wise monotonicity obtained by solving $X_{t+1} = X_t$ and $Y_{t+1} = Y_t$. The curves along which (13) satisfies $\Delta X_t = 0$ and $\Delta Y_t = 0$ are given by the lines

$$Y_t = \ell(X_t) = \frac{r}{\alpha K}(K - X_t) \quad \text{and} \quad X_t = \frac{d}{\gamma}, \tag{20}$$

respectively. We refer to these curves as *nullclines*. Note that these two nullclines are exactly the same as the nullclines obtained for the continuous model (2). These two curves divide the first quadrant into four regions $\mathcal{R}_i$ $(i = 1, 2, 3, 4)$ if $\frac{d}{\gamma} < K$ and three regions otherwise (see Fig. 1). When $d = \gamma K$, the vertical nullcline is the line $x = K$.

We define the regions

$$\mathcal{R}_1 := \left\{ (X_t, Y_t) \in (0, \infty)^2 \colon X_t > \frac{d}{\gamma} \text{ and } Y_t \geq \ell(X_t) \right\},$$

$$\mathcal{R}_2 := \left\{ (X_t, Y_t) \in (0, \infty)^2 \colon X_t \leq \frac{d}{\gamma} \text{ and } Y_t > \ell(X_t) \right\},$$

$$\mathcal{R}_3 := \left\{ (X_t, Y_t) \in (0, \infty)^2 \colon X_t < \frac{d}{\gamma} \text{ and } Y_t \leq \ell(X_t) \right\}, \tag{21}$$

$$\mathcal{R}_4 := \left\{ (X_t, Y_t) \in (0, \infty)^2 \colon X_t \geq \frac{d}{\gamma} \text{ and } Y_t < \ell(X_t) \right\}.$$

For $\gamma K \leq d$, $\mathcal{R}_4 = \emptyset$ and $\mathcal{R}_3 = \{(X_t, Y_t) \in (0, \infty)^2 \colon X_t < K \text{ and } Y_t \leq \ell(X_t)\}$. We emphasize that the interior of $\mathcal{R}_3$ is the set of points $(X_t, Y_t) \in (0, \infty)^2$ such that X_t is increasing and Y_t is decreasing, that is, $\Delta X_t > 0$ and $\Delta Y_t < 0$, and the points on the boundary of $\mathcal{R}_3$ such that $Y_t = \ell(X_t)$ are in $\mathcal{R}_3$, while the points such that $X_t = \frac{d}{\gamma}$ are not in $\mathcal{R}_3$. A similar property, that is, one inequality in the definition of each region is strict and the other is not, holds for all of the regions.

We define the function

$$\mathcal{L}(X_t, Y_t) := Y_{t+1} - \ell(X_{t+1}), \tag{22}$$

where ℓ was defined in (16). If $\mathcal{L}(X_t, Y_t) = 0$, then the point (X_t, Y_t) is mapped to the nullcline $Y_t = \ell(X_t)$. If $\mathcal{L}(X_t, Y_t) > 0$, then the next iterate (X_{t+1}, Y_{t+1}) lies

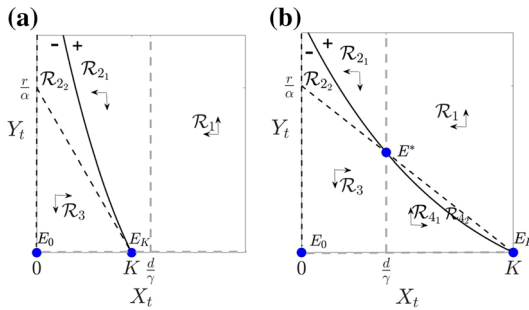**(a)**   **(b)**
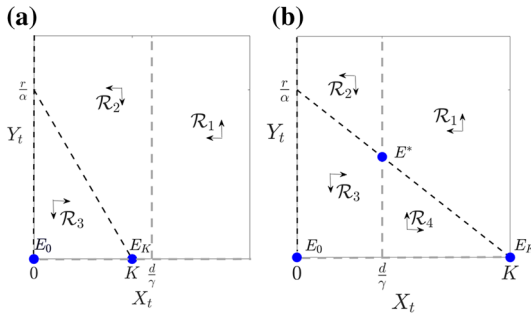
Fig. 1 The phase plane. The gray dashed curves correspond to the predator nullclines and the black dashed curves correspond to the prey nullclines. A horizontal arrow pointing to the right (left) represents $X_{t+1} - X_t > 0$ (< 0) and a vertical arrow pointing up (down) represents $Y_{t+1} - Y_t > 0$ (< 0). Subfigure (**a**) is a schematic image if $\gamma K < d$, while (**b**) shows the case when $\gamma K > d$. Note that in (**a**), there is no region $\mathcal{R}_4$ in the first quadrant

above the nullcline $Y_t = \ell(X_t)$, and if $\mathcal{L}(X_t, Y_t) < 0$, then (X_{t+1}, Y_{t+1}) lies below the nullcline $Y_t = \ell(X_t)$. We call the curve defined implicitly by $\mathcal{L}(X_t, Y_t) = 0$, the *next iterate root-curve associated with the prey nullcline*, or in short *root-curve*. In the case of (13), this curve defines a unique function $\hat{Y}(X_t)$.

Lemma 5 *Consider* (22). *Then there exists a unique positive function* $\widehat{Y}(X_t)$ *such that* $\mathcal{L}(X_t, \widehat{Y}(X_t)) = 0$ *and* $\mathcal{L}(X_t, Y_t) > 0$ *for* $Y_t > \widehat{Y}(X_t)$ *and* $\mathcal{L}(X_t, Y_t) < 0$ *for* $Y_t < \widehat{Y}(X_t)$.

The uniqueness of this root-curve is especially useful for the global analysis. Figure 2 illustrates how to use the root-curve together with the nullclines and the direction field to obtain properties of the solutions. The gray dashed curves correspond to the predator nullclines and the black dashed curves to the prey nullclines. The black solid curve corresponds to $Y_t = \hat{Y}(X_t)$, the next iterate root-curve associated with the prey nullcline. This curve $\hat{Y}(X_t)$ divides the first quadrant into two regions, one above the root-curve where $\mathcal{L}(X_t, Y_t) > 0$, indicated in Fig. 2 by $+$, and the other below the root-curve where $\mathcal{L}(X_t, Y_t) < 0$, indicated by $-$. Any point below the root-curve is mapped below the prey nullcline so that $Y_{t+1} < \ell(X_{t+1})$, and any point above the root-curve is mapped above the prey nullcline. Points on the root-curve are mapped onto the prey nullcline, so that $Y_{t+1} = \ell(X_{t+1})$.

First, consider the case illustrated in Fig. 2a where E_0 and E_K are the only equilibria with both components nonnegative. Since, by Lemma 2, all orbits are bounded, from the direction field in $\mathcal{R}_1$ it follows immediately that no orbit can remain in $\mathcal{R}_1$ indefinitely. Any orbit that visits $\mathcal{R}_1$ must eventually enter $\mathcal{R}_2$ above the nullcline $Y_t = \ell(X_t)$, since $\mathcal{L}(X_t, Y_t) > 0$, as indicated by the $+$ symbol in $\mathcal{R}_1$. From the direction field, in $\mathcal{R}_{2_1} = \mathcal{R}_2 \cap \{Y_t > \hat{Y}(X_t)\}$, any orbit must then either converge to E_K or eventually enter region $\mathcal{R}_{2_2} = \mathcal{R}_2 \backslash \mathcal{R}_{2_1}$. Points in $\mathcal{R}_{2_2}$ are mapped into $\mathcal{R}_3$ in one iteration because of the sign of $\mathcal{L}$ in $\mathcal{R}_{2_2}$, indicated by $-$. In particular, points in the interior of $\mathcal{R}_{2_2}$ are mapped into the interior of $\mathcal{R}_3$, since $\mathcal{L} < 0$. Since the sign of $\mathcal{L}$ is negative for points inside $\mathcal{R}_3$, points in $\mathcal{R}_3$ are mapped below the prey nullcline,

Fig. 2 The phase plane. The gray dashed curves correspond to the predator nullclines and the black dashed curves to the prey nullclines. The black solid curve corresponds to the next iterate *root-curve*, $Y_t = \widehat{Y}(X_t)$, associated with the prey nullcline, $Y_t = \ell(X_t)$. It divides the first quadrant into two regions, the region above the curve where $\mathcal{L}(X_t, Y_t) > 0$ (indicted by $+$) and the region below where $\mathcal{L}(X_t, Y_t) < 0$ (indicated by $-$). Any point in a region where $\mathcal{L}(X_t, Y_t) > 0$ must map to a point above $Y_t = \ell(X_t)$ and any point in a region where $\mathcal{L}(X_t, Y_t) < 0$ must map to a point below $Y_t = \ell(X_t)$. In (**a**), there is no equilibrium with both components positive. The root-curve divides $\mathcal{R}_2$ into sub-regions: $\mathcal{R}_{2_1}$ and $\mathcal{R}_{2_2}$, so that the first quadrant is now divided into four regions. In (**b**), an equilibrium with both components positive, E^*, exists inside the positive quadrant. The root-curve together with the non-trivial nullclines now divide the positive quadrant into six regions: $\mathcal{R}_1, \mathcal{R}_{2_1}, \mathcal{R}_{2_2}, \mathcal{R}_3, \mathcal{R}_{4_1}$, and $\mathcal{R}_{4_2}$

and hence $\mathcal{R}_3$ is positively invariant. Thus, any orbit is trapped in $\mathcal{R}_3$ and the orbit must converge to E_K.

Next, consider the case illustrated in Fig. 2b, in which, in addition to equilibria E_0 and E_K, there is a positive equilibrium, E^*. Reasoning as in the previous case, the direction field together with the positioning of the root-curve indicate that orbits in $\mathcal{R}_1$ must either converge to E^* or, since all solutions are bounded, must eventually enter $\mathcal{R}_2 = \mathcal{R}_{2_1} \cup \mathcal{R}_{2_2}$. No orbit can remain in $\mathcal{R}_{2_1}$ indefinitely due to the direction field and the positioning of the equilibria, but must eventually enter $\mathcal{R}_{2_2}$ due also to the sign of $\mathcal{L}$. Similarly, no orbit can remain in $\mathcal{R}_{4_1}$ indefinitely due to the direction field and the positioning of the equilibria, but must eventually enter $\mathcal{R}_{4_2}$ due also to the sign of $\mathcal{L}$. As well, any orbit in $\mathcal{R}_{2_2}$ is mapped immediately into $\mathcal{R}_3$, and any orbit in $\mathcal{R}_{4_2}$ is mapped immediately into $\mathcal{R}_1$. Any orbit in $\mathcal{R}_3$ must either converge to E^* or eventually enter $\mathcal{R}_4 = \mathcal{R}_{4_1} \cup \mathcal{R}_{4_2}$. Thus, all orbits with positive initial conditions either converge to E^* or cycle indefinitely, entering all four regions at least once in every cycle.

Theorem 6 *If $d \geq \gamma K$, then E_K is globally asymptotically stable with respect to all initial conditions such that $X_0 > 0$ and $Y_0 \geq 0$.*

Theorem 6 states that if the decay rate of the predator exceeds the threshold γK, or equivalently, if the carrying capacity of the prey population is smaller than the ratio of the death rate and consumption-energy rate of the predator population, then the predator goes extinct and the prey population approaches its carrying capacity K. The extinction of the predator population is due to either a large decay rate or due to a low carrying capacity that results in low prey values and hence prevents the predator population from overcoming its decline rate. Based on the discussion in Remark 4,
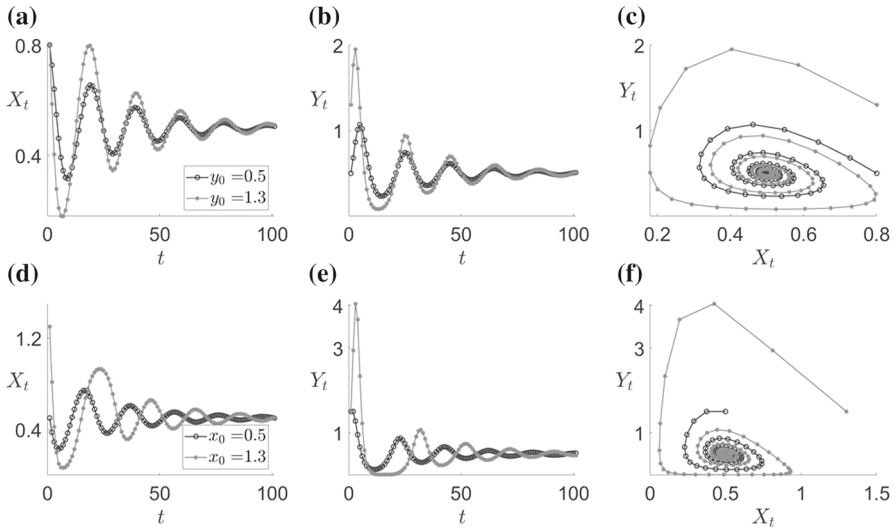
Fig. 3 Simulations using Matlab (MATLAB 2020) for 100 iterations for each pair of initial conditions (X_0, Y_0) and parameters: $r = 0.5$, $K = 1$, $\alpha = 0.5$, $\gamma = 3$, and $d = 1.5$. Note that $1 + d < \gamma K < 1 + 2d$. In (**a**)–(**c**), $X_0 = 0.8$ and the Y_0 values differ. The legends for (**b**) and (**c**) are the same as in (**a**). In (**d**)–(**f**), $Y_0 = 1.5$ and the X_0 values differ. The legends for (**e**) and (**f**) are the same as given in (**d**). In all cases, the orbits spiral towards $E^* = (0.5, 0.5)$

Theorem 6 implies that if the maximal rate of change of the predator is non-positive, then the predator goes extinct.

Theorem 7 *If $d < \gamma K$, then* (13) *is persistent, that is,* $\liminf_{t \to \infty} X_t > 0$ *and* $\liminf_{t \to \infty} Y_t > 0$ *for all solutions with $X_0, Y_0 > 0$.*

Simulations provide support that if $d < \gamma K < 1 + 2d$, then E^* is in fact globally asymptotically stable (see Fig. 3). Independent of the value of the positive initial conditions, solutions converge to the coexistence equilibrium as long as $d < \gamma K < 1 + 2d$. Thus, we believe that E^* is globally asymptotically stable if these parameter inequalities are satisfied and we formulate the following conjecture.

Conjecture 1 *If $d < \gamma K < 1 + 2d$, then E^* is globally asymptotically stable with respect to solutions with positive initial conditions.*

A potential difficulty with respect to proving Conjecture 1 is that no positively invariant rectangle $I := [a_1, b_1] \times [a_2, b_2]$ with $E^* \in I$ exists for (13) because for $(X_t, Y_t) = (b_1, b_2)$, $Y_{t+1} = g(b_1, b_2) = \frac{(1 + \gamma b_1)}{1 + d} b_2 > b_2$, resulting in $(X_{t+1}, Y_{t+1}) \notin I$. However, the following results may contribute to the resolution of Conjecture 1.

Proposition 8 *If $d < \gamma K$ and $(X_0, Y_0) \in (0, \infty)^2$, then there exists $T \geq 0$ such that $X_t < K$ for all $t \geq T$.*

Lemma 9 *If $d < \gamma K$ and $(X_0, Y_0) \in (0, \infty)^2$, then $\limsup_{t \to \infty} X_t \leq K$ and $\limsup_{t \to \infty} Y_t \leq \frac{1 + r}{\alpha} \left(\frac{\gamma K}{d} \cdot \frac{(1 + \gamma K)}{(1 + d)} - 1 \right) =: S$.*
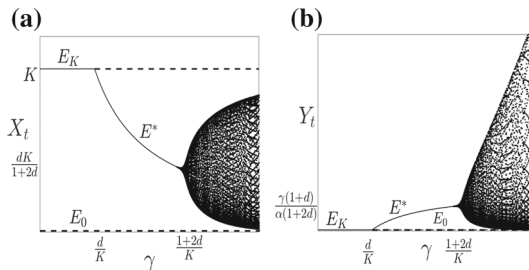
Fig. 4 One-parameter bifurcation diagrams showing how the stability of the equilibria depend on the parameter $\gamma > 0$. Solid curves represent (**a**) the X_t-component and (**b**) the Y_t-component of the stable equilibria and dashed curves the respective unstable component. A transcritical bifurcation occurs when $\gamma = \frac{d}{K}$, where $E_K = E^*$ and a Neimark–Sacker bifurcation occurs when $\gamma = \frac{1+2d}{K}$. These representative diagrams were produced using the same parameter values as in Fig. 3

Proposition 10 *If $d < \gamma K$ and $(X_0, Y_0) \in (0, \infty)^2$, then the only possibilities are*

(a) *(X_t, Y_t) converges to E^* in finite time.*
(b) *There exists $T \in \mathbb{N}$ and $j \in \{1, 3\}$ such that $(X_t, Y_t) \in R_j$ for all $t \geq T$. Then (X_t, Y_t) converges to E^*.*
(c) *Solutions cycle from region $\mathcal{R}_1$ to $\mathcal{R}_2$ to $\mathcal{R}_3$ to $\mathcal{R}_4$ and back to $\mathcal{R}_1$ indefinitely. In each cycle, solutions lie in each region $\mathcal{R}_{2_2}$ and $\mathcal{R}_{4_2}$ exactly once.*

This proposition leads immediately to the following corollary.

Corollary 11 *If $d < \gamma K$ and $(X_0, Y_0) \in (0, \infty)^2$, then there are no orbits with prime period 2 and no orbits with prime period 3.*

Based on Theorem 4, we obtain the bifurcation diagram in Fig. 4. We observe that there are two bifurcations, one when $\gamma K = d$ and the second when $\gamma K = 1 + 2d$.

Theorem 12 *If $d = \gamma K$, then $E_K = E^*$ and (13) undergoes a transcritical bifurcation.*

Theorem 13 *System (13) undergoes a supercritical Neimark–Sacker bifurcation at E^* when $\gamma = \gamma_{\mathrm{crit}} := \frac{1+2d}{K}$. There exists $\delta > 0$ such that a unique stable closed invariant curve bifurcates from the coexistence equilibrium and exists for $\gamma_{\mathrm{crit}} < \gamma < \gamma_{\mathrm{crit}} + \delta$.*

Based on the discussion in Remark 4, this implies that if the maximal rate of change of the predator $g(K)$ exceeds the critical threshold of one, then the prey and predator population converge to a closed curve around the coexistence equilibrium. We illustrate the Neimark–Sacker bifurcation using γ as the bifurcation parameter and the other parameters as in Fig. 3. By Theorem 4, the fixed point E^* is stable when $\frac{d}{K} < \gamma < \frac{1+2d}{K}$ and E^* loses its stability, but remains positive for $\gamma > \frac{1+2d}{K}$. An attractive invariant cycle exists near E^* for $\gamma > \frac{1+2d}{K}$. Bifurcation diagrams in the (γ, x)-plane and the (γ, y)-plane for the above parameters are given in Fig. 4. The corresponding phase portraits are given in Fig. 5. They depict how a smooth invariant cycle bifurcates from the fixed point E^*. We point out that by Lemma 9,

(a)   **(b)**

(c)   **(d)**
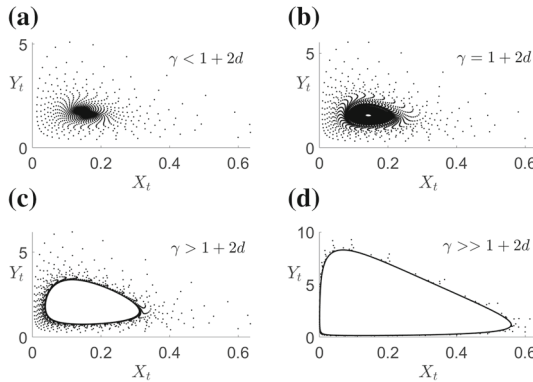
Fig. 5 Phase portraits for (13) with the same parameter values as in Figs. 3 and 4, but different values of γ and 10,000 iterations: in (**a**) $\gamma K = 3 < 1 + 2d$, in (**b**) $\gamma K = 4 = 1 + 2d$ (with 50,000 iterations), in (**c**) $\gamma K = 4.5 > 1 + 2d$, and in (**d**) $\gamma K = 10 >> 1 + 2d$, and initial point $(1.0, 2.0)$. As expected, the convergence is to the unique positive fixed point in (**a**) and in (**b**) and to a closed invariant curve in (**c**) and in (**d**).

the amplitude of the Y-component of the orbit resulting from the Neimark–Sacker bifurcation is bounded by S, a bound independent of the initial conditions. For the specific parameter values in Fig. 3, $S = 6.6$.

It is worth noting that the dynamics of (13) and the dynamics of the continuous predator–prey model with Holling-II functional response,

$$x' = rx\left(1 - \frac{x}{K}\right) - \alpha\frac{x}{1 + \delta x}y, \qquad y' = -dy + \gamma\frac{x}{1 + \delta x}y. \qquad (23)$$

are similar (see for example Sugie and Saito 2012; Wolkowicz 1988; Cheng 1981). Both models (13) and (23) have three equilibria, $E_0 = (0, 0)$, $E_K = (K, 0)$, and a positive equilibrium E^*, (although the components of the positive equilibrium E^* are different). In both models, both components of the third equilibrium, E^*, are positive if and only if $\gamma K > c_1$, where c_1 for each model where c_1 for each model is given in Table 1 and E^* loses stability when γK increases through c_2, where the value of c_2 for each model is also given in Table 1. In both models E_K is asymptotically stable if $\gamma K \in (0, c_1)$ and unstable if $\gamma K > c_1$, and E^* is asymptotically stable if $\gamma K \in (c_1, c_2)$, and unstable if $\gamma K \in (c_2, \infty)$ and when E^* exists and is unstable there is sustained oscillatory behavior. The criteria for stability of the equilibria is summarized in Table 2.

These similarities with our proposed discrete predator–prey model (23) might be explained by recalling that (23) can be derived assuming a handling time, here δ (Dawes and Souza 2013). For larger values of δ, the predator's available time to search for prey is reduced, resulting indirectly in a delay. To some extent, any discrete model may contain an implicit delay as the update of the population is not instant. Additionally, in our model, we specifically exploit that the discrete version of $e^{\int_t^{t+1} p(s)\,ds}$ is $1 + p(t)$ (see (9) and (10)), which can be interpreted as the left-end point approximation and therefore "dating back" to $p(t)$ to model processes for the time interval $(t, t + 1)$.

Table 1 Bifurcation values c_1 and c_2 for the continuous model (23) and our proposed discrete model (13)

	Eq. (23)	Eq. (13)
c_1	$d + \delta K d$	d
c_2	$\delta K d + d + \frac{\gamma}{d}$	$1 + 2d$

Both, (23) and (13) have a tanscritical bifurcation when $\gamma K = c_1$ and a Hopf bifurcation (Neimark–Sacker bifurcation) when $\gamma K = c_2$

Table 2 Stability of the equilibria for the continuous model (23) and our proposed discrete model (13)

γK	$(0, c_1)$	(c_1, c_2)	(c_2, ∞)
E_0	Unstable	Unstable	Unstable
E_K	Stable	Unstable	Unstable
E^*	DNE	Stable	Unstable

Both, (23) and (13) share the same local asymptotic stability of the equilibria for γK in the intervals provided. Here, DNE means that E^* is not biologically meaningful because it is negative

Another interesting relation is observed by recalling the behavior known for the classical Lotka–Volterra predator–prey model, where both species grow/decline exponentially in the absence of the other, and the predator–prey model, where the prey grows logistically. While solutions to

$$x' = rx \left(1 - \frac{x}{K}\right) - \alpha xy, \quad y' = -dy + \gamma xy \tag{24}$$

converge to the unique positive equilibrium for positive initial conditions, the solutions of

$$x' = rx - \alpha xy, \quad y' = -dy + \gamma xy \tag{25}$$

are all closed invariant curves surrounding the unique positive equilibrium with amplitude depending on the initial conditions. Interestingly, if, in our discrete model (13), K exceeds the threshold $\frac{1+2d}{\gamma}$, then solutions also converge to a closed curve. Thus, our model can be considered as intermediate between (24) and (25). This relation may be explained by realizing that the larger K is, the weaker the intraspecific competition, and as $K \to \infty$, (24) approaches (25). Since our derivation method uses a left approximation of exponential contributions due to the zero bond coupon analogy, the effect of intraspecific competition in our model may be weaker than in the continuous model (24).

4 Conclusion

In this work, we derived a discrete predator–prey model baed on the assumption that the prey population grows logistically to a carrying capacity in the absence of the predator population and the predator cannot survive in the absence of the prey population. The derivation is based on expressing the population at time $t + 1$ as a multiple of the

population at time t. This factor was constructed by including the contributions to growth in the numerator and decline processes in the denominator. More precisely, the numerator is expressed as $1 + p(t)$, where p contains the processes contributing to growth, and the denominator is expressed as $1 + q(t)$, where q contains the processes contributing to decline. This formulation resembles a technique known in economic modeling, where the continuous analogue of $1 + p(t)$ is of the form $e^{\int_t^{t+1} p(s)\, ds}$ (see (9) and (10)). The method of deriving the model in this work differs from commonly used methods to obtain discrete models in which discretization schemes such as the Euler scheme are applied to continuous models.

In contrast to some other discretizations of predator–prey systems, the model introduced in this work was derived under the same model assumptions as the well-studied continuous model (2) and exhibits many identical properties. For example, our discrete model (13) satisfies the axiom of parenthood. Also, solutions of (13) with nonnegative initial conditions remain nonnegative and bounded, while other discretizations of (2) with supposedly the same model assumptions, such as (3) and (5), can result in negative solutions. Except for the recurrence (5) that has an additional predator-only equilibrium, the continuous model (2) and the discretizations (3), (4), and our model (13), share the same equilibria structure. That is, each of the four models has two boundary equilibria, namely the trivial and the prey-only equilibrium, as well as (under certain model dependent parameter conditions) one interior equilibrium, the coexistence equilibrium. It is, however, only our recurrence where the nullclines and hence the components of equilibria, as functions of the parameters, are identical to the nullclines and components of the equilibria of (2), with the same interpretation of the parameters.

In both the continuous model and the recurrence introduced in this work, the trivial equilibrium that represents extinction of both populations is unstable. This behavior differs from the discretizations (3) and (5), where parameter values exist for which the zero fixed point is stable. We proved that the prey-only equilibrium of (13) is globally asymptotically stable for the same parameter set as in the continuous case, namely as long as the death rate d of the predator exceeds the threshold γK. Equivalently, if the maximal rate of change of the predator is non-positive, then the predator goes extinct. As the death rate declines below this threshold, the system undergoes a transcritical bifurcation, as is also the case in the continuous model. While, in the continuous model, the coexistence equilibrium is locally asymptotically stable whenever it exists, that is for all $\gamma K > d$, this only remains true for certain parameter values, namely $d < \gamma K < 1 + 2d$ in our discrete model. We also related this stability condition to the value of the maximal rate of change of the predator $g(K)$. If the maximal rate of change of the predator remains below the critical threshold of one(see(19)), populations near the unique positive equilibrium converge to it. Simulations suggest that the coexistence equilibrium of (13) is globally asymptotically stable whenever it is locally asymptotically stable. This is again identical to the dynamics of (2) and significantly differs from the behavior of orbits of the discretizations mentioned in (4), (5), and (3).

The difference in the dynamics predicted between the model introduced here and the analogous continuous model is that there is a supercritical Neimark–Sacker bifur-

cation at the parameter combination, $\gamma K = 1 + 2d$, or equivalently at $g(K) = 1$. Consequently, the coexistence equilibrium remains positive, but loses its local stability and orbits are attracted to a closed curve. Simulations illustrate that even for large γK, orbits converge to a closed curve. While this behavior does not exist in the corresponding continuous predator–prey model (2), Hopf bifurcations are observed in analogous continuous models that differ only when the mass action term is replaced by Holling type II interaction between the prey and the predator (Rosenzweig 1971). In fact, the Holling type II functional response in the continuous predator–prey model can be derived assuming the predator requires time to handle the prey (Dawes and Souza 2013). This reduces the predator growth rate and can be considered as providing an implicit delay.

This cyclic behavior may explain behavior observed in Lotka (1920) who developed a model similar to (2) motivated by their observation of cyclic behavior in nature. While (4) satisfies some desired properties such as nonnegativity of solutions and instability of the trivial solution, it does exhibit chaotic behavior for large r values and therefore differs from the dynamics of the model we presented.

Given the overlap in model assumptions, as well as the similarities in the behavior of the solutions, we believe the discrete predator–prey model introduced in this paper to be the natural discrete analogue of the continuous Lotka–Volterra model with logistic growth in the prey population. The dynamics of the discrete predator–prey model introduced in this work exhibits similarities known from the continuous predator–prey model with Holling type II functional response that assumes a handling time that reduces the predation rate and introduces an implicit delay. We assumed that the decline processes are captured by $(1 + q(t))^{-1}$, which can be understood as the left-point approximation of $\left(e^{\int_t^{t+1} q(s)\,ds} \right)^{-1}$. Thus, the discretization $1 + q(t)$ also contains an implicit time lag when compared to the continuous model. Interestingly, the discrete predator–prey model captures dynamics known for the classical Lotka–Volterra predator–prey model (25), where each species grows exponentially in the absence of each other and solutions are periodic, and the predator–prey model where the prey grows logistically in the absence of the predator and solutions converge to the unique positive equilibrium (24).

The main mathematical contribution of this work lies in the formulation of a discrete phase plane approach to discuss the global dynamics of a planar map. Furthermore, the derivation technique introduced in this paper to construct discrete multi-species models is mathematically and biologically relevant. Here, we specifically applied the method to formulate a predator–prey model, but as mentioned in Sect. 2, it can easily be extended to describe other types of interactions among species. As compared to popular methods of formulating discrete population models, our technique ensures biologically relevant models as the axiom of parenthood and the positivity of solutions with positive initial conditions are satisfied. The interpretation of the stability conditions by introducing the maximal rate of change of the predator provides a biological interpretation of the dynamics.

Declarations

Conflict of interest The authors declare that they have no conflict of interest.

Appendix

In this appendix, we provide the proofs of our results.

Proof of Lemma 2 By Lemma 1, $X_t, Y_t \geq 0$ for nonnegative initial conditions. We first show in (i) that X_t is bounded and then, in (ii), that Y_t is bounded for all $t \geq 0$.

(i) Since f is increasing in the first variable, we have for $X_t \leq K$,

$$X_{t+1} = f(X_t, Y_t) \leq f(K, Y_t) = \frac{(1+r)K}{1+r+\alpha Y_t} \leq K.$$

By (14), for $X_t > K$,

$$X_{t+1} - X_t = X_{t+1}\left[\frac{r}{1+r}\left(1 - \frac{X_t}{K}\right) - \frac{\alpha}{1+r}Y_t\right] < 0. \tag{A1}$$

Hence, X_t decreases for $X_t > K$. Suppose $X_t \geq K$ for all $t \geq 0$. Then X_t is monotone decreasing and therefore convergent. Suppose X_t does not converge to K. Then $\lim_{t\to\infty} X_t = \bar{X} > K$. However, since

$$\bar{X} = \lim_{t\to\infty} X_{t+1} = \lim_{t\to\infty} \frac{(1+r)X_t}{1 + \frac{r}{K}X_t + \alpha Y_t}$$

$$\leq \lim_{t\to\infty} \frac{(1+r)X_t}{1 + \frac{r}{K}X_t} < \frac{(1+r)\bar{X}}{1+r} = \bar{X},$$

this results in a contradiction. Thus, $\bar{X} = K$ if $X_t \geq K$ for all $t \geq 0$. This confirms that for $X_t \geq K$ for all $t \geq 0$, then X_t converges to K. This implies that $X_t \leq \max\{K, X_0\}$ for all $t \geq 0$. This confirms the additional statements in Lemma 2 regarding the X-component of the solution.

(ii) Next we show that Y_t is bounded. We consider two cases: (a) $X_t > K$ for all $t \geq 0$, and (b) there exists $t \geq 0$ such that $X_t \leq K$.

Case (a): We prove that Y_t is bounded using proof by contradiction. By assumption, $X_t > K$ for all $t \geq 0$ and by (i), $\{X_t\}$ decreases monotonically to $\bar{X} = K$. Suppose Y_t is unbounded. Then there exists a subsequence $\{Y_{t_i}\}$ and j such that $Y_{t_i} > 1$ for all $i \geq j$. This, however, implies that for the subsequence X_{t_i+1},

$$X^* = \lim_{t_i\to\infty} X_{t_i+1} = \lim_{t_i\to\infty} \frac{(1+r)X_{t_i}}{1 + r\frac{X_{t_i}}{K} + \alpha Y_{t_i}} \leq \lim_{t_i\to\infty} \frac{(1+r)X_{t_i}}{1 + r\frac{X_{t_i}}{K} + \alpha}$$

$$= \frac{(1+r)X^*}{1 + r\frac{X^*}{K} + \alpha} \leq \frac{(1+r)X^*}{1+r+\alpha} < X^*,$$

resulting in a contradiction. Thus, Y_t is bounded for $t \geq 0$.

Case (b): Without loss of generality, let $j \geq 0$ denote the first iterate such that $X_j \leq K$. Then, by the previous argument, $X_t \leq K$ for all $t \geq j$ and

$$
\begin{aligned}
Y_{t+1} &= \frac{1 + \gamma X_t}{1 + d} Y_t = \frac{1}{1 + d} Y_t + \frac{\gamma}{1 + d} X_t Y_t \\
&= \frac{1}{1 + d} Y_t + \left(\frac{\gamma}{1 + d} \right) \left(\frac{(1 + r) X_{t-1}}{1 + \frac{r}{K} X_{t-1} + \alpha Y_{t-1}} \right) \left(\frac{(1 + \gamma X_{t-1}) Y_{t-1}}{1 + d} \right) \\
&\leq \frac{1}{1 + d} Y_t + \left(\frac{\gamma}{1 + d} \right) \left(\frac{(1 + r) K}{1 + r + \alpha Y_{t-1}} \right) \left(\frac{(1 + \gamma K) Y_{t-1}}{1 + d} \right)
\end{aligned}
$$

for all $t > j$. Consider the recurrence

$$
\hat{Y}_{t+1} = H(\hat{Y}_t, \hat{Y}_{t-1}) = \frac{1}{1 + d} \hat{Y} + A \left(\frac{\hat{Y}_{t-1}}{1 + r + \alpha \hat{Y}_{t-1}} \right),
$$

$$
\text{where} \quad A = \frac{\gamma K (1 + r)(1 + \gamma K)}{(1 + d)^2} > 0, \quad t \geq j, \tag{A2}
$$

with initial condition $\hat{Y}_j = Y_j$ and $\hat{Y}_{j+1} = Y_{j+1}$. We prove by induction that $Y_{t+1} \leq \hat{Y}_{t+1}$ for all $t > j$. Since $\frac{z}{1 + r + \alpha z}$ is increasing in z, we have for $Y_T \leq \hat{Y}_T$ and $Y_{T-1} \leq \hat{Y}_{T-1}$,

$$
\begin{aligned}
Y_{T+1} &\leq \frac{1}{1 + d} Y_T + A \frac{Y_{T-1}}{1 + r + \alpha Y_{t-1}} \\
&\leq \frac{1}{1 + d} \hat{Y}_T + A \frac{\hat{Y}_{T-1}}{1 + r + \alpha \hat{Y}_{T-1}} = \hat{Y}_{T+1},
\end{aligned}
$$

completing the induction argument. To show that Y_t is bounded, it therefore suffices to show that $\hat{Y}_t$ is bounded, that is, there exists $M > 0$ such that for $\hat{Y}_j, \hat{Y}_{j+1} \leq M$, $\hat{Y}_t \leq M$, for all $t > j$. By (A2), $\hat{Y}_{t+1}$ increases in $\hat{Y}_t$ and $\hat{Y}_{t-1}$, and we have

$$
\hat{Y}_{t+1} \leq \frac{1}{1 + d} M + A \frac{M}{1 + r + \alpha M}.
$$

It therefore suffices to show the existence of $M > 0$ such that

$$
\frac{M}{1 + d} + A \frac{M}{1 + r + \alpha M} \leq M.
$$

Solving this inequality for $M > 0$ yields

$$
M \geq \frac{A(1 + d) - (1 + r) d}{d \alpha}. \tag{A3}
$$

Hence, for $\bar{Y} = \max_{i=0,1,\ldots,j,j+1} Y_i$, there exists $M > \max\left\{\bar{Y}, \frac{A(1+d)-(1+r)d}{d\alpha}\right\}$ such that $Y_t \leq M$ for all $t \geq 0$. Thus, Y_t is bounded for all $t \geq 0$ with a bound dependent on the initial conditions X_0, Y_0. This completes the proof. $\qquad\square$

Proof of Lemma 3 (a) Since $f(0, Y_t) = 0$, $X_t = 0$ for all $t \geq 0$ if $X_0 = 0$. In that case, $Y_{t+1} = \frac{1}{(1+d)^t} Y_0$. This converges to zero for $d > 0$. (b) If $Y_0 = 0$, then $Y_t = 0$ for all $t \geq 0$. In the absence of a predator, X_t satisfies a Beverton–Holt recurrence and hence converges to K. $\qquad\square$

Proof of Theorem 4 The Jacobian of system (13) at $(\hat{X}, \hat{Y})$ is given in (18).

(a) The Jacobian at E_0 is

$$J \mid_{(0,0)} = \begin{bmatrix} (1+r) & 0 \\ 0 & \frac{1}{1+d} \end{bmatrix}, \tag{A4}$$

with eigenvalues $\lambda_1 = 1 + r$ and $\lambda_2 = \frac{1}{1+d}$. Since $\lambda_1 > 1$, the trivial equilibrium is unstable.

(b) The Jacobian at E_K is

$$J \mid_{(K,0)} = \begin{bmatrix} \frac{(1+r)}{(1+r)^2} & -\frac{(1+r)\alpha K}{(1+r)^2} \\ 0 & \frac{1+\gamma K}{1+d} \end{bmatrix} = \begin{bmatrix} \frac{1}{1+r} & -\frac{\alpha K}{1+r} \\ 0 & \frac{1+\gamma K}{1+d} \end{bmatrix}. \tag{A5}$$

The eigenvalues of J are $\lambda_1 = \frac{1}{1+r}$ and $\lambda_2 = \frac{1+\gamma K}{1+d}$. Hence, the equilibrium is asymptotically stable if $\gamma K < d$ and unstable if $\gamma K > d$.

(c) At $E^* = (X^*, Y^*)$, using $\beta = \frac{r}{K}(\gamma K - d) > 0$, the Jacobian is

$$J \mid_{(X^*,Y^*)} = \begin{bmatrix} \frac{(1+r)\left(1+\frac{\beta}{\gamma}\right)}{\left(1+\frac{r}{K}\frac{d}{\gamma}+\frac{\beta}{\gamma}\right)^2} & \frac{-(1+r)\alpha\frac{d}{\gamma}}{\left(1+\frac{r}{K}\frac{d}{\gamma}+\frac{\beta}{\gamma}\right)^2} \\ \frac{\gamma\frac{\beta}{\alpha\gamma}}{1+d} & \frac{1+\gamma\frac{d}{\gamma}}{1+d} \end{bmatrix} = \begin{bmatrix} \frac{\left(1+\frac{\beta}{\gamma}\right)}{(1+r)} & \frac{-\alpha d}{\gamma(1+r)} \\ \frac{\beta}{\alpha(1+d)} & 1 \end{bmatrix}, \tag{A6}$$

since the denominators in the first row simplify to $(1 + r)^2$. The characteristic equation is

$$\lambda^2 - \lambda\left(1 + \frac{1+\frac{\beta}{\gamma}}{1+r}\right) + \frac{1+\frac{\beta}{\gamma}}{1+r} + \frac{d\beta}{\gamma(1+r)(1+d)} = 0.$$

Applying the Jury stability test (Ogata 1995, p. 185) to the characteristic equation

$$P(\lambda) = \lambda^2 + a_1\lambda + a_2 \tag{A7}$$

with

$$a_1 = -\left(1 + \frac{1+\frac{\beta}{\gamma}}{1+r}\right), \quad a_2 = \frac{1+\frac{\beta}{\gamma}}{1+r} + \frac{d\beta}{\gamma(1+r)(1+d)},$$

yields the sufficient condition for stability

$$\frac{1 + \frac{\beta}{\gamma}}{1 + r} + \frac{d\beta}{\gamma(1 + r)(1 + d)} < 1.$$

Rearranging yields the equivalent expression

$$(1 + d) + (1 + 2d)\frac{\beta}{\gamma} < (1 + r)(1 + d) \quad \Longleftrightarrow \quad \beta < \gamma\frac{r(1 + d)}{1 + 2d}, \quad \text{(A8)}$$

and recalling $\beta = \frac{r}{K}(\gamma K - d)$, we have

$$\frac{r}{K}(\gamma K - d) < \gamma\frac{r(1 + d)}{1 + 2d} \quad \Longleftrightarrow \quad \gamma < \frac{1 + 2d}{K}.$$

Hence, the coexistence equilibrium is stable if $\gamma K < 1 + 2d$. If instead, $\gamma K > 1 + 2d$, then, by (A8), $\frac{\beta}{\gamma} > \frac{r(1+d)}{1+2d}$ implies

$$(1 + 2d)\frac{\beta}{\gamma} > r(1 + d). \quad \text{(A9)}$$

Thus

$$a_2 = \frac{1 + \frac{\beta}{\gamma}}{1 + r} + \frac{d\frac{\beta}{\gamma}}{(1 + r)(1 + d)} = \frac{1 + d + (1 + 2d)\frac{\beta}{\gamma}}{(1 + r)(1 + d)} \overset{\text{(A9)}}{>} \frac{1 + d + r(1 + d)}{(1 + r)(1 + d)} = 1.$$

We also note that $\beta = \frac{r}{K}(\gamma K - d)$ implies that $\frac{\beta}{\gamma} < r$ since the parameters are positive. Then, $0 < -a_1 = 1 + \frac{1 + \frac{\beta}{\gamma}}{1 + r} < 2$. Thus $a_1^2 - 4a_2 < 0$, implying that $P(\lambda)$ has two complex roots with moduli $\frac{a_1^2 + (4a_2 - a_1^2)}{4} = a_2 > 1$, resulting in the instability of E^*. This completes the proof.

$\square$

Proof of Lemma 5 Let $0 < X_0 < K$, $\mathcal{L}$ be defined as in (22). Using (22) and simplifying the expression, we obtain

$$\mathcal{L}(X_t, Y_t) = Y_{t+1} - \ell(X_{t+1}) = \frac{1 + \gamma X_t}{1 + d}Y_t - \frac{r}{\alpha K}\left(K - \frac{(1 + r)}{1 + \frac{r}{K}X_t + \alpha Y_t}X_t\right)$$

$$= \frac{\alpha K(1 + \gamma X_t)(1 + \frac{r}{K}X_t + \alpha Y_t)Y_t - rK(1 + d)(1 + \frac{r}{K}X_t + \alpha Y_t) + r(1 + d)(1 + r)X_t}{\alpha K(1 + d)(1 + \frac{r}{K}X_t + \alpha Y_t)}$$

$$= \frac{\alpha^2 K(1 + \gamma X_t)Y_t^2 + \left[\alpha K(1 + \gamma X_t)(1 + \frac{r}{K}X_t) - rK(1 + d)\alpha\right]Y_t}{\alpha K(1 + d)(1 + \frac{r}{K}X_t + \alpha Y_t)}$$

$$+ \frac{-rK(1 + d)(1 + \frac{r}{K}X_t) + r(1 + d)(1 + r)X_t}{\alpha K(1 + d)(1 + \frac{r}{K}X_t + \alpha Y_t)}$$

$$= \frac{\sum_{i=0}^{2} c_i Y_t^i}{\alpha(1 + d)(K + rX_t + \alpha KY_t)}, \quad \text{(A10)}$$

with

$$c_0 = r(1+d)(X_t - K),$$
$$c_1 = \alpha(1+\gamma X_t)(K + rX_t) - \alpha rK(1+d),$$
$$c_2 = \alpha^2 K(1+\gamma X_t). \tag{A11}$$

These calculations can be verified using Mathematica (Wolfram Research Inc. 2020).[1] Note that $c_2 > 0$. The sign of $\mathcal{L}(X_t, Y_t)$ is determined by the sign of the numerator in (A10), the quadratic function in the variable Y_t. Although the coefficients c_i are in fact dependent on X_t, $c_0 < 0$, for all $X_t < K$ and $c_2 > 0$ for all $X_t > 0$. Hence, there exists a unique $\widehat{Y}(X_t)$, such that $\sum_{i=0}^{2} c_i Y_t^i < 0$ for $0 < Y_t < \widehat{Y}(X_t)$ and $\sum_{i=0}^{2} c_i Y_t^i > 0$ for $\widehat{Y}(X_t) < Y_t$. This completes the first claim. Replacing Y_t by $\ell(X_t)$ in (22), we have

$$\alpha(1+d)(K + rX_t + \alpha K\ell(X_t)) = \alpha(1+d)\left(K + rX_t + \alpha K\frac{r}{\alpha K}(K - X_t)\right)$$
$$= \alpha(1+d)K(1+r)$$

and

$$c_0 + c_2\ell^2(X_t) + c_1\ell(X_t)$$
$$= r(1+d)(X_t - K) + \alpha^2 K(1+\gamma X_t)\left(\frac{r}{\alpha K}(K - X_t)\right)^2$$
$$+ \alpha(1+\gamma X_t)(K + rX_t)\frac{r}{\alpha K}(K - X_t) - \alpha rK(1+d)\frac{r}{\alpha K}(K - X_t)$$
$$= r(1+d)(X_t - K) + (1+\gamma X_t)\frac{r^2}{K}(K - X_t)^2$$
$$+ (1+\gamma X_t)r(K - X_t) + (1+\gamma X_t)X_t\frac{r^2}{K}(K - X_t) - r^2(1+d)(K - X_t)$$
$$= r(1+d)(X_t - K)(1+r) + (1+\gamma X_t)\frac{r^2}{K}(K - X_t)(K - X_t + X_t)$$
$$+ (1+\gamma X_t)r(K - X_t)$$
$$= r(1+d)(X_t - K)(1+r) + (1+\gamma X_t)r^2(K - X_t) + (1+\gamma X_t)r(K - X_t)$$
$$= r(1+d)(X_t - K)(1+r) + (1+\gamma X_t)r(K - X_t)(1+r)$$
$$= (1+r)r(K - X_t)(-(1+d) + (1+\gamma X_t)).$$

Thus,

$$\mathcal{L}(X_t, \ell(X_t)) = \frac{\sum_{i=0}^{2} c_i\ell^i(X_t)}{\alpha(1+d)(K + rX_t + \alpha K\ell(X_t))}$$

---

[1] The expression for $\mathcal{L}(X, Y)$ can be obtained by the Mathematica command: $T = \text{Together}[(1 + \gamma *X)/(1 + d) * Y - r/(\alpha * K) * (K - (1 + r)/(1 + r/K * X + \alpha * Y) * X)]$ The coefficients c_i can be obtained by the command: Simplify[Coefficient[Numerator[T],Y,i]] for $i = 0, 1, 2$.

$$= \frac{(1+r)r(K - X_t)(-(1+d) + (1+\gamma X_t))}{\alpha(1+d)K(1+r)}$$

$$= \frac{r(K - X_t)(\gamma X_t - d)}{\alpha(1+d)K}. \tag{A12}$$

The expression can be verified using Mathematica (Wolfram Research Inc. 2020).[2] □

Proof of Theorem 6 Let $X_0, Y_0 > 0$. When $d \geq \gamma K$, the set of nonnegative equilibria in the first quadrant is $\mathcal{E} = \{E_0, E_K\}$. Without loss of generality, assume that $X_0 < K$, since for $X_0 > 0$, by Lemma 2, X_t either converges to K, so that (X_t, Y_t) converges to E_K, or there exists $T > 0$ such that $X_t < K$ for all $t \geq T$. If $d \geq \gamma K$, the nullclines defined in (20) divide phase space into the three regions $\mathcal{R}_i$ ($i = 1, 2, 3$) (see Fig. 1b). Observe that

(a) If $(X_t, Y_t) \in \mathcal{R}_1$ for all $t \geq 0$, by the boundedness of solutions proved in Lemma 2 and the monotonicity ($X_{t+1} < X_t$ and $Y_{t+1} > Y_t$), the solution must converge to a point in $\mathcal{E}$. However, since the Y_t-component of the points in $\mathcal{E}$ are zero, but the Y_t-component of the sequence of iterates is increasing for all points in $\mathcal{R}_1$, this is impossible, and hence the solution must eventually enter $B_{12} \cup \mathcal{R}_2 \cup B_{23} \cup \mathcal{R}_3$.
(b) Let $(X_t, Y_t) \in \mathcal{R}_2$. If (X_t, Y_t) remains in $\mathcal{R}_2$ indefinitely, then (X_t, Y_t) converges to E_K. Otherwise, by the direction field, there exists $T > 0$ with $(X_T, Y_T) \in \mathcal{R}_3$.
(c) If $(X_t, Y_t) \in \mathcal{R}_3$, then $X_t < K$ and therefore, $X_{t+1} < K$ so that $(X_{t+1}, Y_{t+1}) \notin \mathcal{R}_1$. We now show that $(X_{t+1}, Y_{t+1}) \notin \mathcal{R}_2$, and hence must remain in $\mathcal{R}_3$. By Lemma 5 iii), there exists a unique positive $\hat{Y}(X_t)$ such that $\sum_{i=0}^{2} c_i Y_t^i$ changes sign at $Y_t = \hat{Y}(X_t)$ and $\sum_{i=0}^{2} c_i Y_t^i > 0$ for all $Y_t > \hat{Y}_t(X_t)$. Furthermore, since $\mathcal{L}(X_t, \ell(X_t)) < 0$ by (A12) for $X_t < K < \frac{d}{\gamma}$, Y_{t+1} remains below the line $\ell(X_t)$. Thus, (X_t, Y_t) remains in the interior of $\mathcal{R}_3$ and converges to E_K. Therefore, in all cases, solutions converge to E_K.

We provide an alternative proof for $d > \gamma K$ using a Lyapunov function. If $X_t \geq K$ for all t, then by Lemma 2, X_t converges to K and by (b), $\lim_{t \to \infty} Y_t = 0$. Assume now, without loss of generality, that $X_0 < K$. We claim that

$$V(X_t, Y_t) = (X_t - K)^2 + cY_t, \quad \text{where} \quad c = 4\frac{\alpha K^2(1+d)}{\gamma(1+r)\left(\frac{d}{\gamma} - K\right)} > 0$$

is a Lyapunov function for (13). Clearly, $V(K, 0) = 0$ and $V(X_t, Y_t) > 0$ for $(X_t, Y_t) \neq (K, 0)$. Next, we show that $\Delta V(X_t, Y_t) < 0$.

$$\Delta V(X_t, Y_t) = V(X_{t+1}, Y_{t+1}) - V(X_t, Y_t)$$
$$= X_{t+1}^2 - 2X_{t+1}K - X_t^2 + 2X_t K + c(Y_{t+1} - Y_t)$$
$$= (X_{t+1} - X_t)(X_{t+1} + X_t - 2K) + c(Y_{t+1} - Y_t),$$

---

[2] The expression for $\mathcal{L}(X, \ell(X))$ can be obtained by using T found via the Mathematica command in footnote 1: Simplify$[T/.Y - > r/(alpha * K) * (K - X)]$

so that $\Delta V(K, 0) = 0$. Replacing $X_{t+1} - X_t$ and $Y_{t+1} - Y_t$ with (14) and (15) yields

$$
\begin{aligned}
\Delta V(X_t, Y_t) &= (X_{t+1} - X_t)(X_{t+1} + X_t - 2K) + c(Y_{t+1} - Y_t) \\
&= X_{t+1}\left(\frac{r}{1+r}\left(1 - \frac{X_t}{K}\right) - \frac{\alpha}{1+r}Y_t\right)(X_{t+1} + X_t - 2K) + c\frac{\gamma}{1+d}Y_t\left(X_t - \frac{d}{\gamma}\right) \\
&= \frac{r}{1+r}X_{t+1}\left(1 - \frac{X_t}{K}\right)(X_t - K) + \frac{r}{1+r}X_{t+1}\left(1 - \frac{X_t}{K}\right)(X_{t+1} - K) \\
&\quad - \frac{\alpha}{1+r}X_{t+1}Y_t(X_t - K) - \frac{\alpha}{1+r}X_{t+1}Y_t(X_{t+1} - K) + c\frac{\gamma}{1+d}Y_t\left(X_t - \frac{d}{\gamma}\right) \\
&= \frac{-r}{K(1+r)}X_{t+1}(K - X_t)^2 - \frac{r}{K(1+r)}X_{t+1}(K - X_t)(K - X_{t+1}) \\
&\quad - Y_t\left(c\frac{\gamma}{1+d}\left(\frac{d}{\gamma} - X_t\right) - \frac{\alpha}{1+r}X_{t+1}(K - X_t) - \frac{\alpha}{1+r}X_{t+1}(K - X_{t+1})\right).
\end{aligned}
$$

The first two terms are negative, since by Lemma 2, $0 < X_t < K$ for all $t \geq 0$. Furthermore,

$$
\begin{aligned}
h(X_t) &:= c\frac{\gamma}{1+d}\left(\frac{d}{\gamma} - X_t\right) - \frac{\alpha}{1+r}X_{t+1}(K - X_t) - \frac{\alpha}{1+r}X_{t+1}(K - X_{t+1}) \\
&> 4\frac{\alpha K^2(1+d)}{\gamma(1+r)\left(\frac{d}{\gamma} - K\right)}\left(\frac{\gamma}{1+d}\left(\frac{d}{\gamma} - K\right)\right) - 2\frac{\alpha}{1+r}K^2 > 0,
\end{aligned}
$$

completing the proof using (Kelley and Peterson 2001, Theorem 4.18), if $d > \gamma K$. □

Proof of Theorem 7 Assume that $d < \gamma K$. We verify the assumptions (B1)–(B6) and (H1)–(H3) in (Freedman and So 1989, Theorem 3.3).

(B1) Let $\mathbb{R}_+^2 = \{(x, y) \in \mathbb{R}^2 : x \geq 0, y \geq 0\}$. Then consider the metric space $\langle \mathbb{R}_+^2, \tilde{d} \rangle$ with the Euclidean metric $\tilde{d}$.

(B2) Let the set $\partial \mathbb{R}_+^2 = \{(x, y) \in \mathbb{R}_+^2 : xy = 0\}$, that is, the boundary of $\mathbb{R}_+^2$. Then $\partial \mathbb{R}_+^2$ is a closed subset of $\mathbb{R}_+^2$.

(B3) $(f, g) : \mathbb{R}_+^2 \to \mathbb{R}_+^2$ is continuous, where f and g are defined in (13).

(B4) By Lemma 1, $(f, g)(\partial \mathbb{R}_+^2) \subset \partial \mathbb{R}_+^2$.

(B5) By Lemma 1, $(f, g)(\mathbb{R}_+^2 \setminus \partial \mathbb{R}_+^2) \subset \mathbb{R}_+^2 \setminus \partial \mathbb{R}_+^2$.

(B6) By Lemma 2, the closure of any positive orbit through any $(X_0, Y_0) \in \mathbb{R}_+^2$ is compact.

(H1) $(f, g)|_{\partial \mathbb{R}_+^2}$ is dissipative since any orbit with $X_0 = 0$ and $Y_0 \geq 0$ converges to E_0 and any point with $X_0 > 0$ and $Y_0 = 0$ converges to E_K.

(H2) $(f, g)|_{\partial \mathbb{R}_+^2}$ has acyclic covering $\{E_0, E_K\}$.

(H3) From the local stability analysis given in the proof of Theorem 4, E_0 and E_K are both saddles and each has a one-dimensional stable manifold. In particular, the stable manifold of E_0 is $W^+(E_0) = \{(x, y) \in \partial \mathbb{R}_+^2 : x = 0\}$, and the stable manifold of E_K is $W^+(E_K) = \{(x, y) \in \partial \mathbb{R}_+^2 : x > 0\}$, and hence $W^+(E_0) \cap \mathbb{R}_+^2 \setminus \partial \mathbb{R}_+^2 = \emptyset$ and $W^+(E_K) \cap \mathbb{R}_+^2 \setminus \partial \mathbb{R}_+^2 = \emptyset$.

Since all of the hypotheses of (Freedman and So 1989, Theorem 3.3) are satisfied, (13) is persistent. □

Proof of Proposition 8 Assume $d < \gamma K$. If $X_t \leq K$ and $Y_t > 0$, then $X_{t+1} = \frac{(1+r)X_t}{1+\frac{r}{K}X_t+\alpha Y_t} < \frac{(1+r)X_t}{1+\frac{r}{K}X_t} \leq X_t \leq K$, so that $X_{t+1} < K$. Assume now that $X_t > K$ for all $t \geq 0$. Then, by (14) and (A1), X_t is monotone decreasing for $K \leq X_{t+1} < X_t$. Also, since $X_t > K > \frac{d}{\gamma}$, by (15), Y_t is monotone increasing. Thus, $Y_t > Y_0 > 0$ and $\bar{X} := \lim_{t\to\infty} X_t \geq K$ exists. Suppose $\bar{X} \geq K$. Then,

$$\bar{X} = \lim_{t\to\infty} X_{t+1} = \lim_{t\to\infty} \frac{(1+r)X_t}{1+\frac{r}{K}X_t+\alpha Y_t} \leq \lim_{t\to\infty} \frac{(1+r)X_t}{1+\frac{r}{K}X_t+\alpha Y_0} = \frac{(1+r)\bar{X}}{1+\frac{r}{K}\bar{X}+\alpha Y_0}.$$

Therefore, $1+r\frac{\bar{X}}{K}+\alpha Y_0 \leq 1+r$, or equivalently, $\alpha Y_0 \leq r\left(1-\frac{\bar{X}}{K}\right) \leq 0$, contradicting $Y_0 > 0$. □

Proof of Lemma 9 Assume that $d < \gamma K$ and $(X_0, Y_0) \in (0, \infty)^2$. By Lemma 2, X_t, Y_t are bounded for $t \geq 0$. The claim $\limsup_{t\to\infty} X_t \leq K$ follows immediately from Lemma 2. By Lemma 1, since $Y_0 > 0$, $Y_t > 0$ for all $t \geq 0$. Thus, there exists $T \geq 0$ such that $X_t < K$ for all $t \geq T$, since otherwise, if $X_t \geq K$ for all $t \geq 0$, then $(X_t, Y_t) \in \mathcal{R}_1 \cup \{(X_t, Y_t): X_t = K\}$ indefinitely. This is, however, not possible, since Y_t is bounded by Lemma 2. By the direction field, this implies that there exists T such that $(X_T, Y_T) \in \mathcal{R}_2$, and therefore $X_T \leq K$. Note that if $X_T = K$, then since $Y_T > 0$, $X_{T+1} < K$. Therefore, there exists $T \geq 0$ such that $X_T < K$. Recall that the boundedness of Y_t was obtained by proving an upper bound for the upper solution $\hat{Y}_t$, where $\hat{Y}_t$ satisfies (A2). To show that $\limsup_{t\to\infty} Y_t$ is uniformly bounded, it suffices to prove there is a unique value $\bar{Y}$ such that all solutions of the upper solution of (A2) converge to $\bar{Y}$, since then, for $U \geq \bar{Y}$, $\limsup_{t\to\infty} \hat{Y}_t = \lim_{t\to\infty} \hat{Y}_t = \hat{Y}^* \leq U$, and the claim is justified. The map H in (A2) satisfies

$$\frac{\partial H(u, v)}{\partial u} = \frac{1}{1+d} > 0, \quad \frac{\partial H(u, v)}{\partial v} = \frac{A(1+r)}{(1+r+\alpha v)^2} > 0$$

and is therefore component-wise monotone and (strictly) increasing in both variables. For M defined in (A3), $\hat{Y}_t \leq M$ for all $t \geq 0$ as long as $0 \leq \hat{Y}_0, \hat{Y}_1 \leq M$. Note that for $\gamma K > d$,

$$A(1+d) - d(1+r) = \frac{\gamma K(1+r)(1+\gamma K)}{(1+d)} - d(1+r)$$
$$> \frac{d(1+r)(1+d)}{(1+d)} - d(1+r) = 0,$$

and therefore $M > 0$. Furthermore, for $0 < m \leq \frac{A(1+d)-d(1+r)}{d\alpha}$,

$$\hat{Y}_{t+1} = H(\hat{Y}_t, \hat{Y}_{t-1}) \geq H(m, m) = \frac{m}{1+d} + \frac{Am}{1+r+\alpha m}$$

$$= m \left(1 + \frac{A(1+d)}{(1+d)(1+r+\alpha m)} \right)$$

$$\geq m \left(1 + \frac{A(1+d)}{(1+d)(1+r+\alpha \frac{A(1+d)-d(1+r)}{d\alpha})} \right)$$

$$= m \left(1 + \frac{A(1+d)}{(1+d)\frac{A(1+d)}{d}} \right) > m.$$

Thus, $H : [m, M] \to [m, M]$. To apply (Grove and Ladas 2004, Theorem 1.15), we note that the only solution $(s, S) \in [m, M]$ of

$$s = H(s, s), \quad S = H(S, S)$$

is $s = S = s^* = \frac{A(1+d)-d(1+r)}{\alpha d} > 0$ and $s^* \in [m, M]$. Thus, by (Grove and Ladas 2004, Theorem 1.15), s^* is globally attracting, and therefore $\lim_{t\to\infty} \hat{Y}_t = s^* = \frac{A(1+d)-d(1+r)}{\alpha d}$. Choosing $U > s^*$ results in $\limsup_{t\to\infty} Y_t \leq \limsup_{t\to\infty} \hat{Y}_t = \lim_{t\to\infty} \hat{Y}_t = s^* < U$. $\qquad \square$

Proof of Proposition 10 Let $\mathcal{R}_i$, $i = 1, 2, 3, 4$, be the regions defined in (21) (see Fig. 1b). Lemma 5 and (22) will also be used to prove Theorem 10. Define $\mathcal{E} = \{E_0, E_K, E^*\}$, the set of equilibria of (13).

(a) Clearly one possibility is that the solution converges to E^* in finite time, e.g., the solution with $(X_0, Y_0) = E^*$.

(b) We show that if the solution remains in the single region $\mathcal{R}_j$, $j = 1$ or $j = 3$, for all sufficiently large t, then it must converge to E^*. Assume that there exists $j \in \{1, 3\}$ and $T > 0$ such that $(X_t, Y_t) \in \mathcal{R}_j$ for all $t \geq T$.

  - If $j = 1$, that is, there exists T such that $(X_t, Y_t) \in \mathcal{R}_1$ for all $t \geq T$, then by boundedness and monotonicity, the solution must converge to a point in $\mathcal{E}$. Given the direction field in $\mathcal{R}_1$, the orbit converges to E^*.
  - If $j = 3$, that is, there exists T such that $(X_t, Y_t) \in \mathcal{R}_3$ for all $t \geq T$, then again by monotonicity and boundedness, the solution must converge to a point in $\mathcal{E}$. Given the direction field in $\mathcal{R}_3$, the orbit converges to E^*.

(c) First we show that the solution cannot remain in $\mathcal{R}_2$ for all sufficiently large t or in $\mathcal{R}_4$ for all sufficiently large t. Suppose there exists $T > 0$ such that $(X_t, Y_t) \in \mathcal{R}_2$ for all $t \geq T$. Then due to the monotonicity and boundedness of solutions, by Lemma 2, in this region, the solution would have to converge to a point in $\mathcal{E}$. The intersection of $\mathcal{E}$ with the closure of $\mathcal{R}_2$ contains only E^*. Since, in $\mathcal{R}_2$, $X_{t+1} < X_t < X^*$, for all $t \geq T$, convergence to E^* is impossible. Similarly, suppose there exists $T > 0$ such that $(X_t, Y_t) \in \mathcal{R}_4$ for all $t \geq T$. Then the solution is bounded and monotone, and hence it must converge to a point in $\mathcal{E}$. The intersection of $\mathcal{E}$ with the closure of $\mathcal{R}_4$ contains only $\{E_K, E^*\}$. Since, for all $t \geq T$, in $\mathcal{R}_4$, $Y_{t+1} \geq Y_t > 0$, convergence to E_K is impossible and since $X_{t+1} > X_t > \frac{d}{\gamma} = X^*$, convergence to $E^* = (X^*, Y^*)$ is also impossible.

Assume now that the solution (X_t, Y_t) of (13) does not converge to E^* in finite time nor does it eventually remain in one of the four regions, $\mathcal{R}_i$ for $i = 1, 2, 3, 4$. We now show that it must enter each of the four regions indefinitely.

Since $X_t < K$, for all sufficiently large t, we assume, without loss of generality, that $X_0 < K$.

- If $(X_t, Y_t) \in \mathcal{R}_1$, then we show that (X_{t+1}, Y_{t+1}) must be above the line $Y_t = \ell(X_t)$. For $(X_t, Y_t) \in \mathcal{R}_1$, $\ell(X_t) \leq Y_t$ and $X_t > X^*$. By (A12), $\mathcal{L}(X_t, \ell(X_t)) > 0$ and since $c_2 > 0$ by (A11), by Lemma 5 (iii), $\mathcal{L}(X_t, Y_t) > 0$ for all $Y_t \geq \ell(X_t)$. Thus, $Y_{t+1} > \ell(X_{t+1})$, so that $(X_{t+1}, Y_{t+1}) \in \mathcal{R}_1 \cup \mathcal{R}_2$. Since by assumption, this solution does not remain in a single region, there exists T such that $(X_T, Y_T) \in \mathcal{R}_1$ and $(X_{T+1}, Y_{T+1}) \in \mathcal{R}_2$.
- If $(X_t, Y_t) \in \mathcal{R}_2$, then $X_{t+1} < X_t < X^*$, and by the direction field in $\mathcal{R}_2$, (see Fig. 1b) as well as the assumption that solutions do not remain in a single region indefinitely, there exists $T \geq t$ such that $(X_T, Y_T) \in \mathcal{R}_2$ and $(X_{T+1}, Y_{T+1}) \in \mathcal{R}_3$. This specifically implies that $(X_T, Y_T) \in \mathcal{R}_{2_2}$ since $\mathcal{L}(X_t, Y_t)$ must be nonpositive for the next iterate to be in $\mathcal{R}_3$. Note that two subsequent iterates cannot be in $\mathcal{R}_{2_2}$ because $\mathcal{L}(X_T, Y_T) \leq 0$ in $\mathcal{R}_{2_2}$.
- If $(X_t, Y_t) \in \mathcal{R}_3$, then we show that (X_{t+1}, Y_{t+1}) must be below the line $Y_t = \ell(X_t)$. If $(X_t, Y_t) \in \mathcal{R}_3$, then $0 < Y_t \leq \ell(X_t)$. Since $X_t < X^*$, by (A12), $\mathcal{L}(X_t, \ell(X_t)) < 0$, and therefore, by Lemma 5 (iii), $\mathcal{L}(X_t, Y_t) < 0$ for all $0 < Y_t \leq \ell(X_t)$. Thus, $Y_{t+1} < \ell(X_{t+1})$ and $(X_{t+1}, Y_{t+1}) \in \mathcal{R}_3 \cup \mathcal{R}_4$. By assumption, the solution does not remain in a single region indefinitely, and given the direction field, there exists T such that $(X_T, Y_T) \in \mathcal{R}_3$ and $(X_{T+1}, Y_{T+1}) \in \mathcal{R}_4$.
- If $(X_t, Y_t) \in \mathcal{R}_4$, then by the monotonicity of each component of the solution in that region (see Fig. 1b) the solution does not remain in $\mathcal{R}_4$. Thus, there exists T such that $(X_T, Y_T) \in \mathcal{R}_4$ and $(X_{T+1}, Y_{T+1}) \in \mathcal{R}_1$. This specifically implies that $(X_T, Y_T) \in \mathcal{R}_{4_2}$ since $\mathcal{L}(X_t, Y_t)$ must be nonnegative for the next iterate to be in $\mathcal{R}_1$. Note that two subsequent iterates cannot be in $\mathcal{R}_{4_2}$ because $\mathcal{L}(X_T, Y_T) \geq 0$ in $\mathcal{R}_{4_2}$.

Therefore, in case (c), the solution rotates counterclockwise about E^*, entering each region $\mathcal{R}_i$ for $i = 1, 2, 3, 4$, indefinitely. Furthermore, the solutions lie in $\mathcal{R}_{2_2}$ and $\mathcal{R}_{4_2}$ exactly once in each cycle. This completes the proof. □

Proof of Theorem 12 For $d = \gamma K$, the equilibria E_K and E^* coalesce. The Jacobian evaluated at E_K given in (A5) has eigenvalues $\lambda_1 = \frac{1}{1+r}$ and $\lambda_2 = 1$. As well, the branches E_K and E^* are unique and exchange stability as γ passes through $\frac{d}{\gamma}$, that is, when $d - \gamma K$ changes sign. Thus, there is a transcritical bifurcation. □

Proof of Theorem 13 Define $\beta = \frac{r}{K}(K\gamma - d)$. For $\gamma = \frac{1+2d}{K}$, $\frac{\beta}{\gamma} = r\frac{1+d}{1+2d}$. The characteristic equation obtained for the Jacobian about E^* given in (A6) when $\gamma_{\text{crit}} = \frac{1+2d}{K}$ is

$$\lambda^2 - B\lambda + C = \lambda^2 - \lambda\left(1 + \frac{1 + r\frac{1+d}{1+2d}}{(1+r)}\right) + \frac{1 + r\frac{1+d}{1+2d}}{1+r} + \frac{rd\frac{1+d}{1+2d}}{(1+r)(1+d)}$$

$$= \lambda^2 - \lambda \left(1 + \frac{1 + r \frac{1+d}{1+2d}}{(1 + r)} \right) + 1 = 0,$$

and

$$B^2 - 4C = \left(1 + \frac{1 + r \frac{1+d}{1+2d}}{(1 + r)} \right)^2 - 4 = \frac{-rd(7rd + 8d + 4(r + 1))}{(1 + 2d)^2 (1 + r)^2} < 0.$$

Hence, when $\gamma = \gamma_{\text{crit}}$, the two eigenvalues are complex with $\|\lambda\|^2 = C = 1$. The characteristic equation for the coexistence equilibrium at E^* for $\gamma = \gamma_{\text{crit}} + \delta$ was given in (A7), that is, $\lambda^2 + a_1 \lambda + a_2 = 0$ with

$$a_1 = - \left(1 + \frac{1 + \frac{\beta}{\gamma}}{1 + r} \right) \quad \text{and} \quad a_2 = -(a_1 + 1) + \frac{d \frac{\beta}{\gamma}}{(1 + d)(1 + r)}.$$

The eigenvalues in polar form are $\lambda = R(\gamma) e^{\pm i \theta(\gamma)}$, where $R(\gamma) = \sqrt{a_2(\gamma)}$ and

$$R'(\gamma_{\text{crit}}) = \frac{a_2'(\gamma_{\text{crit}})}{2\sqrt{a_2(\gamma_{\text{crit}})}} = x$$

$$= \frac{1}{2\sqrt{a_2(\gamma_{\text{crit}})}} \frac{(1 + 2d)}{(1 + d)(1 + r)} \left(\frac{\beta'(\gamma)\gamma - \beta(\gamma)}{\gamma^2} \right) |_{\gamma = \gamma_{\text{crit}}}.$$

Since $a_2(\gamma_{\text{crit}}) = 1$ and $\beta'(\gamma)\gamma - \beta(\gamma) = \frac{r}{K}d \neq 0$, the first degeneracy condition is satisfied. To show that the second is also satisfied, note that $\tan(\theta_0) = \frac{\sqrt{4a_2 - a_1^2}}{(-a_1)}$ and $e^{ki\theta_0} \neq 1$ for $k = 1, 2, 3, 4$ for $r, d > 0$. Hence there is a Neimark–Sacker bifurcation at $\gamma = \gamma_{\text{crit}}$. In order to use the formula in Guckenheimer and Holmes (1983) to determine the criticality of the bifurcation, we translate E^* to the origin. Let

$$W_t := X_t - X^* = X_t - \frac{d}{\gamma} \quad \text{and} \quad Z_t := Y_t - Y^* = Y_t - \frac{\beta}{\alpha\gamma}.$$

Then, (13) in the variables of W_t, Z_t becomes

$$W_{t+1} = h_1(W_t, Z_t, \gamma), \quad Z_{t+1} = h_2(W_t, Z_t, \gamma),$$

where

$$h_1(w, z, \gamma) := -\frac{d}{\gamma} + \frac{(1 + r)\left(\frac{d}{\gamma} + w\right)}{1 + \frac{r}{K}w + r + \alpha z},$$

$$h_2(w, z, \gamma) := -\frac{\beta}{\alpha\gamma} + \frac{\left(1 + \gamma\left(\frac{d}{\gamma} + w\right)\right)\left(\frac{\beta}{\alpha\gamma} + z\right)}{1 + d}.$$

(A13)

The Jacobian of (A13) at $(W_t, Z_t, \gamma) = (0, 0, \gamma_{\text{crit}})$ is given by

$$
J_{(0,0,\gamma_{\text{crit}})} = \begin{bmatrix} \frac{1+2d+r(1+d)}{(1+2d)(1+r)} & \frac{-\alpha d K}{(1+2d)(1+r)} \\ \frac{r}{K\alpha} & 1 \end{bmatrix}
$$

with eigenvalues

$$
\lambda_1 = \underbrace{\frac{(2+4d+2r+3dr)}{2(1+2d)(1+r)}}_{\lambda_{11}} + i \underbrace{\frac{\sqrt{dr(4+8d+4r+7dr)}}{2(1+2d)(1+r)}}_{\lambda_{12}},
$$

and λ_2, the complex conjugate of λ_1. The corresponding eigenvectors are

$$
\mathbf{v}_{\lambda_1} = \underbrace{\begin{pmatrix} \frac{-\alpha d K}{2(1+2d)(1+r)} \\ 1 \end{pmatrix}}_{\mathbf{U}_1} + i \underbrace{\begin{pmatrix} \frac{\alpha K \sqrt{dr(4+8d+4r+7dr)}}{2r(1+2d)(1+r)} \\ 0 \end{pmatrix}}_{\mathbf{U}_2},
$$

and $\mathbf{v}_{\lambda_2}$, the complex conjugate of $\mathbf{v}_{\lambda_1}$. Define the matrix $T := \begin{bmatrix} \mathbf{U}_2 & \mathbf{U}_1 \end{bmatrix}$. Applying the transformation $(u, v)^T = T^{-1}(w, z)^T$, where

$$
T^{-1} = \begin{pmatrix} \frac{2r(1+2d)(1+r)}{\alpha K \sqrt{dr(4+8d+4r+7dr)}} & \frac{dr}{\sqrt{dr(4+8d+4r+7dr)}} \\ 0 & 1 \end{pmatrix},
$$

yields

$$
\begin{pmatrix} u_{t+1} \\ v_{t+1} \end{pmatrix} = \begin{bmatrix} \lambda_{11} & -\lambda_{12} \\ \lambda_{12} & \lambda_{11} \end{bmatrix} \begin{pmatrix} u_t \\ v_t \end{pmatrix} + \begin{pmatrix} F(u, v) \\ G(u, v) \end{pmatrix}.
$$

The nonlinear terms are

$$
F(u, v) = \frac{dv\alpha(u\sqrt{dr(4+8d+4r+7dr)} - drv)}{2(1+d)(1+r)\sqrt{dr(4+8d+4r+7dr)}} - \frac{N}{D}
$$

$$
G(u, v) = \frac{\alpha v(u\sqrt{dr(4+8d+4r+7dr)} - drv)}{2r(1+d)(1+r)},
$$

where

$$
N = 2\alpha(u\sqrt{dr(4+8d+4r+7dr)} + v(2+4d+2r+3dr)) \times
$$
$$
\times \, (u\sqrt{dr(4+8d+4r+7dr)}(1+r+d(2+r)) - vdr(3+6d+3r+5dr))
$$
$$
D = 2(1+r)\left(dr(4+8d+4r+7dr)[(1+2d)(2+2r^2+\alpha\sqrt{dr(4+8d+4r+7dr)}u \right.
$$
$$
\left. +2\alpha v+2r(2+\alpha v)+d(4+4r^2+4\alpha v+r(8+3\alpha v)))] \right)^{\frac{1}{2}}.
$$

According to the formula in Guckenheimer and Holmes (1983) and Iooss and Joseph (1980), the criticality of the bifurcation at $\gamma = \gamma_{\text{crit}}$ is determined by the sign of

$$\varphi = -\text{Re}\left[\frac{(1-2\lambda)\bar{\lambda}^2}{1-\lambda}\xi_{11}\xi_{20}\right] - \frac{1}{2}\|\xi_{11}\|^2 - \|\xi_{02}\|^2 + \text{Re}(\bar{\lambda}\xi_{21}),$$

where

$$\xi_{20} = \frac{1}{8}\left(F_{uu} - F_{vv} + 2G_{uv} + i(G_{uu} - G_{vv} - 2F_{uv})\right)|_{(0,0)},$$

$$\xi_{11} = \frac{1}{4}\left(F_{uu} + F_{vv} + i(G_{uu} + G_{vv})\right)|_{(0,0)},$$

$$\xi_{02} = \frac{1}{8}\left(F_{uu} - F_{vv} - 2G_{uv} + i(G_{uu} - G_{vv} + 2F_{uv})\right)|_{(0,0)},$$

$$\xi_{21} = \frac{1}{16}\left(F_{uuu} + F_{uvv} + G_{uuv} + G_{vvv} + i(G_{uuu} + G_{uvv} - F_{uuv} - F_{vvv})\right)|_{(0,0)}.$$

Since

$$\varphi = -\frac{\alpha^2 d(2(1+r) + 4d^2(1+r) + d(6+5r))}{8(1+d)^2(1+2d)(1+r)^3} < 0,$$

the Neimark–Sacker bifurcation at $\gamma = \gamma_{\text{crit}}$ is supercritical.   □

References

Beddington J, Free C, Lawton J (1975) Dynamic complexity in predator–prey models framed in difference equations. Nature 255:58–60

Beddington J, Free C, Lawton J (1978) Characteristics of successful natural enemies in models of biological control of insect pests. Nature 273:513–519

Beverton RJH, Holt SJ (1957) On the dynamics of exploited fish populations, vol. 19 of Fishery Investigations (Great Britain, Ministry of Agriculture, Fisheries, and Food), H. M. Stationery Off., London

Bohner M, R C (2013) The Beverton–Holt q-difference equation. J Biol Dyn 7(1):86–95

Bohner M, Stević S, Warth H (2007) The Beverton–Holt difference equation. Discrete Dyn Differ Equ, pp 189–193

Bohner M, Streipert SH (2016) Optimal harvesting policy for the Beverton–Holt model. Math Biosci Eng 13(4):673–695

Bohner M, Streipert SH (2017) The second Cushing–Henson conjecture for the Beverton-Holt q-difference equation. Opuscula Math 37(6):795–819

Bohner M, Warth H (2007) The Beverton–Holt dynamic equation. Appl Anal 86(8):1007–1015

Brauer F, Castillo-Chavez C (2011) Mathematical models in population biology and epidemiology. Texts in applied mathematics. Springer, New York

Chen X-W, Fu X-L, Jing Z-J (2013) Complex dynamics in a discrete-time predator-prey system without Allee effect. Acta Math Appl Sin 29:355–376

Chen X-W, Fu X-L, Jing Z-J (2013) Dynamics in a discrete-time predator-prey system with Allee effect. Acta Math Appl Sin 29:143–164

Cheng KS (1981) Uniqueness of a limit cycle for a predator-prey system. SIAM J Math Anal 12(4):541–548

Choudhury S (1992) On bifurcations and chaos in predator–prey models with delay. Chaos Solitons Fract 2:393–409

Dawes JHP, Souza MO (2013) Mathematical of Holling's type I, II and III functional responses in predator–prey systems. J Theoret Biol 237:11–22

Din Q (2013) Dynamics of a discrete Lotka–Volterra model. Adv Differ Equ 2013, Article 95

Edelstein-Keshet L (1988) Mathematical models in biology, classics in applied mathematics. Society for Industrial and Applied Mathematics, (SIAM, 3600 Market Street, Floor 6, Philadelphia, PA 19104)

Fan M, Agarwal S (2002) Periodic solutions of nonautonomous discrete predator–prey system of Lotka–Volterra type. Appl Anal 81:801–812

Fazly M, Hesaaraki M (2008a) Periodic solutions for a semi-ratio-dependent predator-prey dynamical system with a class of functional responses on time scales. Discrete Contin Dyn Syst Ser B 9(2), 267–279

Fazly M, Hesaaraki M (2008b) Periodic solutions for predator–prey systems with Beddington–Deangelis functional response on time scales. Nonlinear Anal Real World Appl 9(3):1224–1235

Freedman HI, So JW-H (1989) Persistence in discrete semidynamical systems. SIAM J Appl Math 20(4):930–938

Grove EA, Ladas G (2004) Periodicities in nonlinear difference equations. Advances in discrete mathematics and applications. CRC Press, Boca Raton, FL

Guckenheimer J, Holmes P (1983) Nonlinear oscillations, dynamical systems, and bifurcations of vector fields, vol 42 of Appl. Math. Sci., 2 edn. Springer, New York

He Z, Li B (2014) Complex dynamic behavior of a discrete-time predator–prey system of Holling-III type. Adv Differ Equ 2014:180

Hirsch MW, Smith H (2005) Monotone maps: a review. J Differ Equ Appl 11(4–5):379–398

Hutchinson G (1978) An introduction to population ecology. Yale University Press, New Haven

Iooss G, Joseph D (1980) Elementary stability and bifurcation theory. Undergraduate texts in mathematics. Springer, New York

Kangalgil F, Isik S (2020) Controlling chaos and Neimark–Sacker bifurcation in a discrete-time predator–prey system. Hacet J Math Stat 49(5):1761–1776

Kelley W, Peterson A (2001) Difference equations: an introduction with applications. Elsevier Science, Cambridge

Khan AQ, Ahmad I, Alayachi HS, Noorani MSM, Khaliq A (2020) Discrete-time predator–prey model with flip bifurcation and chaos control. Math Biosci Eng 17(5):5944–5960

Kingsland S (1995) Modeling nature. Science and its conceptual foundations series. University of Chicago Press, Chicago

Kot M (2001) Elements of mathematical ecology. Cambridge University Press, Cambridge

Liu P, Elaydi SN (2001) Discrete competitive and cooperative models of Lotka–Volterra type. J Comput Anal Appl 3(1):53–73

Lotka AJ (1920) Analytical note on certain rhythmic relations in organic systems. Proc Natl Acad Sci USA 6(7):410–415

MATLAB (2020) version R2020b. The MathWorks Inc., Natick, MA

May R (1974) Biological populations with nonoverlapping generations: stable points, stable cycles, and chaos. Science 186:4164

Mickens RE (1989) Exact solutions to a finite-difference model of a nonlinear reaction–advection equation: implications for numerical analysis. Numer Methods Partial Differ Equ 5(4):313–325

Mickens RE (1994a) Genesis of elementary numerical instabilities in finite-difference models of ordinary differential equations. In: Proceedings of dynamic systems and applications, vol 1 (Atlanta, GA, 1993), Dynamic, Atlanta, GA, pp 251–257

Mickens RE (1994) Nonstandard finite difference models of differential equations. World Scientific, River Edge, NJ

Mickens RE, Smith A (1990) Finite-difference models of ordinary differential equations: influence of denominator functions. J Frankl Inst 327(1):143–149

Ogata K (1995) Discrete-time control systems. Prentice Hall, Upper Saddle River

Rana SMS (2019) Bifurcations and chaos control in a discrete-time predator–prey system of Leslie type. J Appl Anal Comput 9(1):31–44

Rosenzweig M (1971) The paradox of enrichment. Science 171(3969):385–387

Rozikov UA, Shoyimardonov SK (2020) Leslie's prey–predator model in discrete time. Int J Biomath 13(6):2050053

Smith HL, Thieme HR (2013) Persistence and global stability for a class of discrete time structured population models. Discrete Contin Dyn Syst 33:4627

Sugie J, Saito Y (2012) Uniqueness of limit cycles in a Rosenzweig–MacArthur model with prey immigration. SIAM J Appl Math 72(1):299–316

Verhulst P-F (1838) Notice sur la loi que la population suit dans son accroissement. Corr Math Phy 10:113–121

Volterra V (1926) Variazioni e fluttuazioni del numero d'individui in specie animali conviventi. Mem Acad Lincei Roma 2:31–113

Wang W, Jiao Y, Chen X (2013) Asymmetrical impact of Allee effect on a discrete-time predator–prey system. J Appl Math 2013:1–10

Wiggins S (2003) Introduction to applied nonlinear dynamical systems and chaos. Texts in applied mathematics. Springer, New York

Wolfram Research Inc. (2020) Mathematica 12.2

Wolkowicz GSK (1988) Bifurcation analysis of a predator–prey system involving group defence. SIAM J Appl Math 48(3):592–606

Zhang W (2006) Discrete dynamical systems, bifurcations and chaos in economics, mathematics in science and engineering. Elsevier, Amsterdam

Zhang W, Bi P, Zhu D (2008) Periodicity in a ratio-dependent predator–prey system with stage-structured predator on time scales. Nonlinear Anal Real World Appl 9(2):344–353

Zhao M, Xuan Z, Li C (2016) Dynamics of a discrete-time predator–prey system. Adv Differ Equ 191:1–8